land

Article

Reduction of Fine Dust and Alleviation of Heat Island Effect: An Analysis of Cold Air Flow in Pohang City, South Korea

Woonkun Jung and Gunwoo Kim *

Graduate School of Urban Studies, Hanyang University, 222 Wangsimni-ro, Seongdong-gu, Seoul 04763, Republic of Korea; sunfls21@hanyang.ac.kr
* Correspondence: gwkim1@hanyang.ac.kr; Tel.: +82-2-2220-0274

Abstract: The urban heat island (UHI) effect poses a significant challenge for cities like Pohang, South Korea, which suffer from environmental pollution. Integrating a ventilation corridor into city planning can mitigate this issue. Despite wind's potential as a resource for urban areas, its role remains under-studied in urban planning and design. To address this gap, this study analyzes the wind environment of Pohang City to identify effective strategies for reducing the UHI effect through the implementation of wind corridors, thereby enhancing the city's thermal environment and sustainability. We used the KLAM_21 model to simulate and analyze the cold airflow. The results indicate that the land cover of Pohang, including residential and commercial areas, consists of urbanized dry areas. The wind direction over the past 10 years (2013–2022) has generally been west–southwest (247.5°). The cold air height and flow direction range expanded around the Hyeongsan River, eventually affecting the central city after 5 h. In the simulations, cold air accumulated above 30 m at specific locations near the valley's base. After 2 h, the flow range of the cold air height increased. The green area ratio (GAR) and cold air speed positively correlated (+0.153). Thus, creating a wind-corridor forest could effectively address Pohang's fine dust and UHI phenomena.

Keywords: Pohang-si; cold air; flow analysis; fine dust; urban heat island; wind corridor; KLAM_21 model; South Korea; correlation analysis; green area ratio (GAR)

Citation: Jung, W.; Kim, G. Reduction of Fine Dust and Alleviation of Heat Island Effect: An Analysis of Cold Air Flow in Pohang City, South Korea. *Land* **2024**, *13*, 347. https://doi.org/10.3390/land13030347

Academic Editor: Guoyu Ren

Received: 31 January 2024
Revised: 27 February 2024
Accepted: 6 March 2024
Published: 8 March 2024

1. Introduction

There is growing interest in developing wind corridors for cold air to reduce fine dust and alleviate the urban heat island (UHI) effect to improve the atmospheric environments of urban regions. A wind corridor of cold air refers to a path through which wind blows in a city; it facilitates the circulation of cold and fresh air generated at night from forests in the outskirts of a city to the center of a city, thereby reducing air pollution and improving the thermal environment of the city [1]. Cold air is more easily generated in fields or meadows than in forests, but forest areas are more suitable as wind corridors because cold air can flow down the slopes of these areas into surrounding villages [2]. Notably, 63% of the Korean territory consists of forested lands, with mountains and forests close to cities. Thus, forest areas can be used as wind corridors to reduce the UHI effect in nearby urban regions.

The generation of cold air begins around 20:00 h, when radiant heat starts to cool down after sunset, reaching the peak between 4:00 h and 6:00 h in the following morning before sunrise [3]. As trees release oxygen at night through respiration, the air temperature in forests is 5–9 °C lower than that in cities. Several studies have shown that cold and heavy air in forests flows down valleys at night, forcing the hot and polluted air in cities upwards and diffusing air pollutants toward the outskirts.

The concept of a wind corridor was first proposed by Gunther Kress (1979) [4], who combined "ventilation" with the German word "bahn" (which means "train") and created the term "ventilationbahn". Currently, it refers to facilitating fresh air flow from mountains or oceans toward cities, using a network of greens and open spaces, city, and water [5].

Notably, this approach has been employed in urban planning in Germany as the importance of city climate has grown. Wind corridors are designed to ensure that cold (Kaltluft) and fresh (Frischluft) air can smoothly flow into urban areas; these designs are based on the elements of creating and using a wind corridor in urban planning processes, as an effort to mitigate environmental problems, such as air pollution and the UHI phenomenon [6].

The tropical night phenomenon refers to the air in urban regions being drier during the daytime compared with that in natural areas while exhibiting reversed conditions at night [7]. Such climatic characteristics affect the distribution of night air in large cities while influencing the so-called tropical night phenomenon. Furthermore, hot and humid vapor generated in urbanized areas can combine with highly polluted air to form clouds; ultimately, the vapor falls back into the entire city and induces a hot and humid urban environment [8]. Various methods have been implemented across different fields to resolve the UHI effect and fine dust problems in cities, such as using roadside trees as green infrastructure, rooftop or wall greening, and waterscape facilities or winds. Different methods involving waterscape spaces, such as water fountains, waterfalls, streams, and ponds, or tree planting, such as horizontal and vertical greening, can solve environmental problems in narrow spaces. However, these methods fail to consider the entirety of a city.

Several similar studies have also been conducted in other countries; Weiwu Wang et al. (2022) [9] examined the heat island phenomenon in Hangzhou and discovered that 54 high-temperature and 48 low-temperature zones were identified as functional and compensation spaces in Hangzhou, respectively. Mostafa Gholipour Gashniani et al. (2022) [10] investigated the optimal procedure for utilizing wind energy for natural ventilation in buildings in Manjil, Iran, by applying double-skin façades as a novel renewable energy source. Kangkang Gu et al. (2020) [11] analyzed the introduction of an effective modeling method for urban ventilation corridors. Federica Marando et al. (2022) [12] proposed a model for lowering heat intensity and high city temperatures. Jeong-min Son et al. (2022) [13] analyzed the characteristics of local cold air based on various spatial characteristics. Uk-je Sung et al. (2021) [14] investigated the use of wind-corridor forests in Korean cities.

Furthermore, Jae-gyu Cha (2010) [15] proposed a wind flow analysis and evaluation method. Bo-yong Seo (2022) [16] evaluated cold airflow with respect to the development of public housing complexes and investigated legal and systematic improvements in the region while targeting the Yeongyeong public housing district in Daegu. Soo-bong Kim et al. (2004) [17] proposed the development of a wind corridor of cold air as an improvement measure for reducing the heat island phenomenon in Daegu. Jeong-hee Eum (2019) [18] suggested an effective approach for dealing with summer weather in Daegu by conducting a study on introducing and forming a wind corridor to mitigate the UHI effect. Including the study by Eum, nine studies focused primarily on the utilization of wind corridors. Since 2020, most studies have focused on wind corridors and thermal environments. Jong-sung Kim and Jung-eun Kang (2021) [19] identified the city of Changwon as a vulnerable region requiring thermal environment improvement and studied the region's formation plan for a wind corridor. In addition, Ho-yeong Moon et al. (2021) [20] analyzed different wind corridor characteristics to improve the thermal environment of Busan Metropolitan City and proposed a relevant management strategy. Despite the growing research in urban wind corridors, there persists a notable gap in fully evaluating their effectiveness, and the application of city-scale approaches remains limited. Consequently, this study aims to address this gap by conducting a comprehensive analysis of the city's wind environment, proposing effective wind corridors that can mitigate the urban heat island effect and enhance the overall environmental quality of the city.

Additionally, the influence of built-up areas on urban heat islands has been explored in several studies. Lin, Wei, and Guan (2024) [21] emphasized the significance of improving the land use pattern within built-up areas to mitigate the UHI phenomenon, utilizing morphological spatial pattern analysis (MSPA) to characterize land use configuration, revealing that the morphological characteristics of built-up areas significantly affect UHI intensity, with a suggested arrangement of key morphological categories to lessen negative influences on land surface temperature. Similarly, Zheng, Han, and Keeffe (2024) evaluated outdoor thermal comfort in Shenzhen. They found that ground-level arboreal elements contribute most to thermal comfort enhancement, underscoring the significance of considering microclimatic concerns during urban design [22]. Furthermore, Lin et al. (2023) utilized the local climate zone system to analyze the impact of building morphology and spatial distribution on seasonal land surface temperatures (LST) in Fuzhou. Their findings highlight the importance of building morphology, with different building forms exerting varying degrees of influence on LST levels [23]. These studies underscore the importance of strategic urban planning and design interventions, informed by detailed analysis of built environment characteristics, in mitigating the adverse effects of UHIs and improving urban thermal comfort.

The industrial structure of Pohang mainly consists of the steel industry and related gray infrastructure and processes, which can harm public health and deteriorate local air quality owing to the large amounts of air pollutants emitted annually. In particular, the compactness of residential and industrial areas further deteriorates environmental quality as perceived by local residents [24]. Furthermore, air pollution and the UHI phenomenon are exacerbated by atmospheric stagnation in towns located close to industrial areas. Cold air generated from the forests on the city's outskirts does not flow into these towns but instead flows along the 450 m wide Hyeongsan River toward the ocean. Similarly, the UHI phenomenon in Pohang has severely affected the city. Therefore, the significance of this study lies in suggesting the need to improve its thermal environment. We propose a practical strategy for reducing the UHI effect by analyzing the flow of cold air. This study aims to answer the following research question: Based on the current situation of the wind environment in Pohang City, what strategies can be employed to mitigate the impacts of fine dust and the urban heat island (UHI) phenomenon through the implementation of wind corridors on a city-wide scale?

2. Materials and Methods

2.1. Study Area

We selected Pohang City as the major target area, and a portion of Gyeongju City was also included in the study, covering a total of 900 km^2 (30 km $\times$ 30 km). The longitude and latitude of Pohang are 129.36° E and 36.00° N, respectively (Figure 1). The city is surrounded by mountains, with northeastern Pohang on the coast. The water system comprises the Hyeongsan River and Naengcheon Stream (which pass through the study area and penetrate the city) and the Yongyeon, Angye, and Wangshinji reservoirs. Notably, neighborhood parks are located within the city and are surrounded by several mountains, including the Unjesan, Doeumsan, and Sambongsan Mountains (Figure 2).

2.2. Methods

We examined the major wind corridors in Pohang by analyzing the flow of cold air. The environmental characteristics of the study area were reviewed during the survey and analysis of the current state. First, relevant data on the study area's terrain, water systems, and green areas were collected and preprocessed to analyze the region's natural environment (Table A1). Data on land coverage and transportation were also collected and preprocessed to analyze the demographics and social environment of the region. We collected and preprocessed temperature, wind direction, and wind speed data to analyze the region's climate. Furthermore, we analyzed the cold air characteristics and modeled a wind corridor in the study area.

Figure 1. Location of Pohang City, South Korea.

Figure 2. Topography (**left**), the water system (**middle**), and green spaces (**right**) of the study area.

Second, we investigated the current state of urban wind-corridor forests and examined their correlation with wind flow using meteorological observatories 1 ASOS (Automated Surface Observing System) 1 and 1 AWS (Automatic Weather Station). Basic data were constructed and processed before a simulation analysis of the changes in the wind flow was performed. Furthermore, we analyzed the characteristics and flow of cold air at night in the study area using the KLAM_21 model (a cold air flow analysis model). Subsequently, changes in the height and flow of cold air were analyzed before and after applying the solution, which consisted of operating a water curtain at the Hyeongsan Big Bridge (POSCO Bridge). To analyze the urban wind-corridor forests, we built relevant geographic information system (GIS) data for each forest type within the study area. For analyzing the correlation between cold airspeed and the ratio of urban wind-corridor forest area by the grid, we measured the Pearson correlation after matching the green area ratio (GAR) data by a grid with the data of cold airspeed. Figure 3 shows a flowchart illustrating the steps implemented to analyze the cold air flow in Pohang.

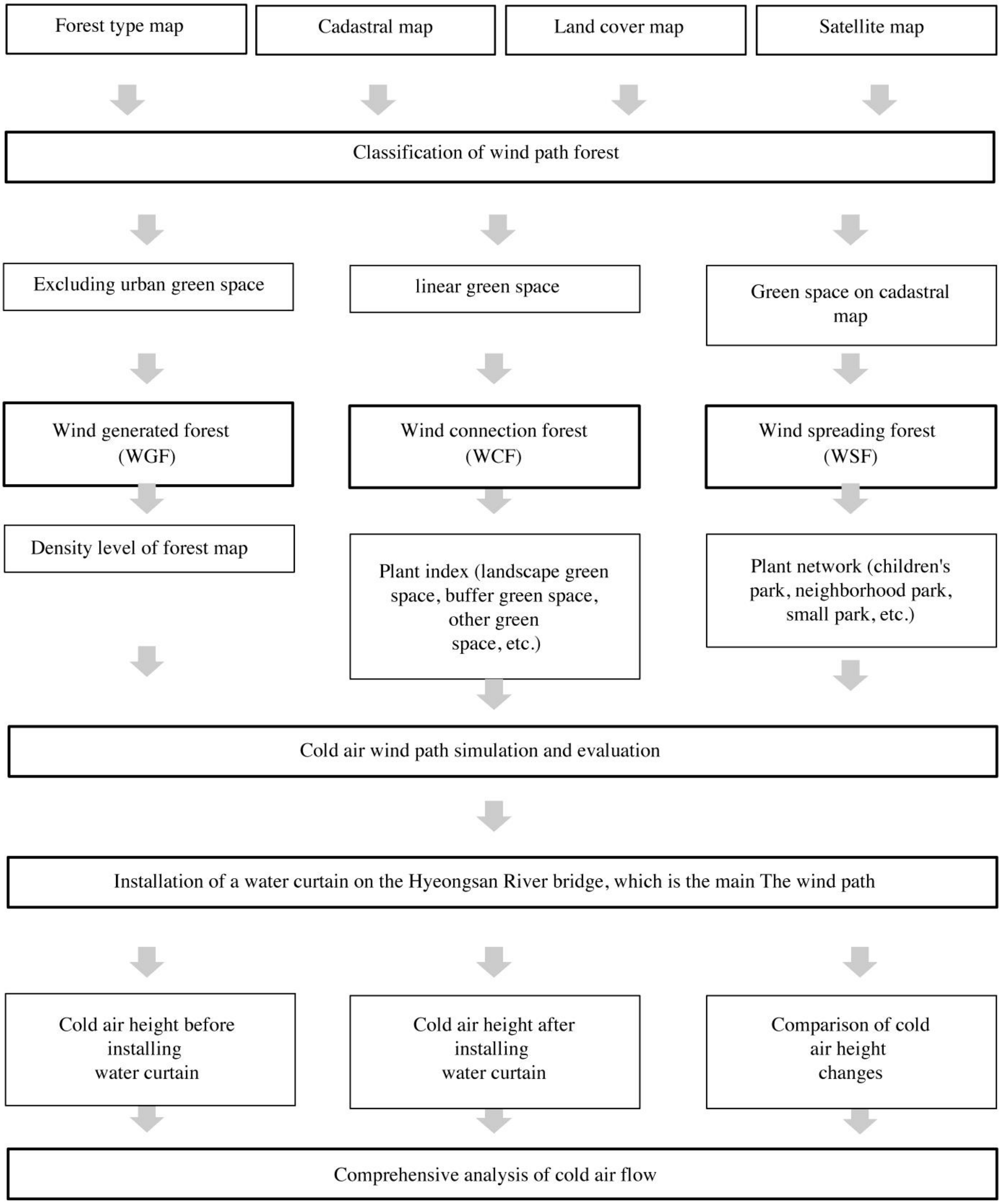

Figure 3. Flowchart portraying the steps implemented to analyze the cold air flow in Pohang.

2.3. Analysis Tool

First, KLAM_21 was used to analyze the generation and flow of cold air in the study area and surrounding regions. KLAM_21 is a two-dimensional, mathematical-physical urban microclimate model created by the German Meteorological Service (Deutscher Wetterdienst), which analyzes the generation, accumulation, and flow of cold air at night based on various input information such as land use, terrain shape, and roughness. The model's physical framework comprises simplified equations of motion and energy balance, enabling the determination of energy loss and the "cold content" of the cold air layer. This cold content informs the calculation of cold air height for each column, considering height-dependent cooling. The model outputs the spatial distribution of cold air height, along with mean flow velocity or volume flows available at any given time. Comparisons between actual and planned states are visualized using difference maps or temporal animations, showcasing cold air height, flow velocity, or volume flows. Unlike simplistic models, KLAM_21 captures cold air movements dynamically and temporally, offering a detailed representation of their dynamics and evolution [25]. Alternative methods like computational fluid dynamics offer high resolution but may require greater resources, while statistical approaches may lack detailed resolution. Notably, the model was capable of simulating up to 1500 × 1500 grids. Second, data on terrain and land use were required to perform simulations using KLAM_21, and data on buildings were crucial for analyzing the effects of buildings. For the terrain data, numerical maps provided on the National Geographic Information Platform (National Geographic Information Institute, Suwon Special City, Republic of Korea) were used to extract the intermediate and index contours, and a digital elevation model (DEM) was created using GIS and converted into ASCII code for use as input in KLAM_21. For land use, we collected coverage maps provided by the Environment Spatial Information Service (Ministry of Environment), which were reclassified as appropriate for KLAM_21 and converted into the ASCII code for input in KLAM_21. Third, because KLAM_21 is based on German standards and does not necessarily reflect the characteristics of cities in other countries, the land cover code was changed to fit the spatial characteristics of South Korea. For buildings, numerical maps available on the National Geographic Information Platform (National Geographic Information Institute) were used to extract the latest information on buildings and the road name address (Ministry of the Interior and Safety), which were then converted into ASCII code for use as inputs in KLAM_21.

The conditions for analyzing the data using KLAM_21 were as follows: the analysis range was 30 km × 30 km, grid spacing was 20 m, and grids were 1500 × 1500. The initial input values (weather conditions) were set, as shown in Table 1, based on the weather data of the study area.

Table 1. Initial input values for the analysis.

Category	Wind Speed	Wind Direction	Simulation Time
Initial input values	2.67 m/s	West–southwest (247.5°)	Duration of 10 h From 20:00 (sunset) h to 06:00 h of the following day
	Average wind speed and most frequent wind direction over the past 10 years (2013–2022)		

3. Results

3.1. Analysis of Generation and Flow of Cold Air

3.1.1. Simulation of Cold Air Speed and Flow Direction

To analyze the general wind environment of the study area, the speed and flow direction of the cold air generated in the study area were modeled hourly for 10 h. After 1 h (approximately 21:00), cold air generated from nearby mountains flowed into the valley's base, corresponding to the spatial characteristics of the terrain, and the cold air speed increased gradually. The cold air speed was ≤0.2 m/s in most regions, but it reached

0.5 m/s at slopes, streams (Hyeongsan River), and main roads. After 2 h (around 22:00 h), the cold airspeed increased, especially at points in a valley start and along the Hyeongsan River; the cold air speed was ≥1 m/s. After 3 h (approximately 23:00 h), the cold air speed increased consistently in most regions. The cold air speed increased further downstream of the Hyeongsan River (≥3 m/s); the cold air flowed along the stream quickly, traveling toward the East Sea. After 4 h (approximately 24:00), cold air consistently flowed along the Hyeongsan River, partially affecting the city. The cold air speed was ≤0.2 m/s in most parts of the city, while the speeds near the roads were 0.2–0.5 m/s. After 5 h (01:00–06:00 h), the cold airspeed gradually decreased with simulation time. In contrast, cold air flowed consistently and quickly along the Hyeongsan River, indicating that the river passing through Pohang was the major wind corridor in the region. The simulation results of the cold air speed and flow direction indicated that the cold air generated near the mountainous regions (Doeumsan and Unjesan mountains) after sunset quickly moved along the valley, stream, and into the city. During the early hours of the simulation, the cold air speed generally decreased, except when it flowed close to the Hyeongsan River; however, the inflow of cold air continued around the stream, which implied that the stream was the major wind-corridor region of Pohang. The physical properties of cold air mean that it tends to flow from a higher elevation to a lower elevation owing to its higher density than hot air, accumulates in the lower ground near the stream, and gradually expands its range. Figure 4 shows a graphical representation of the results.

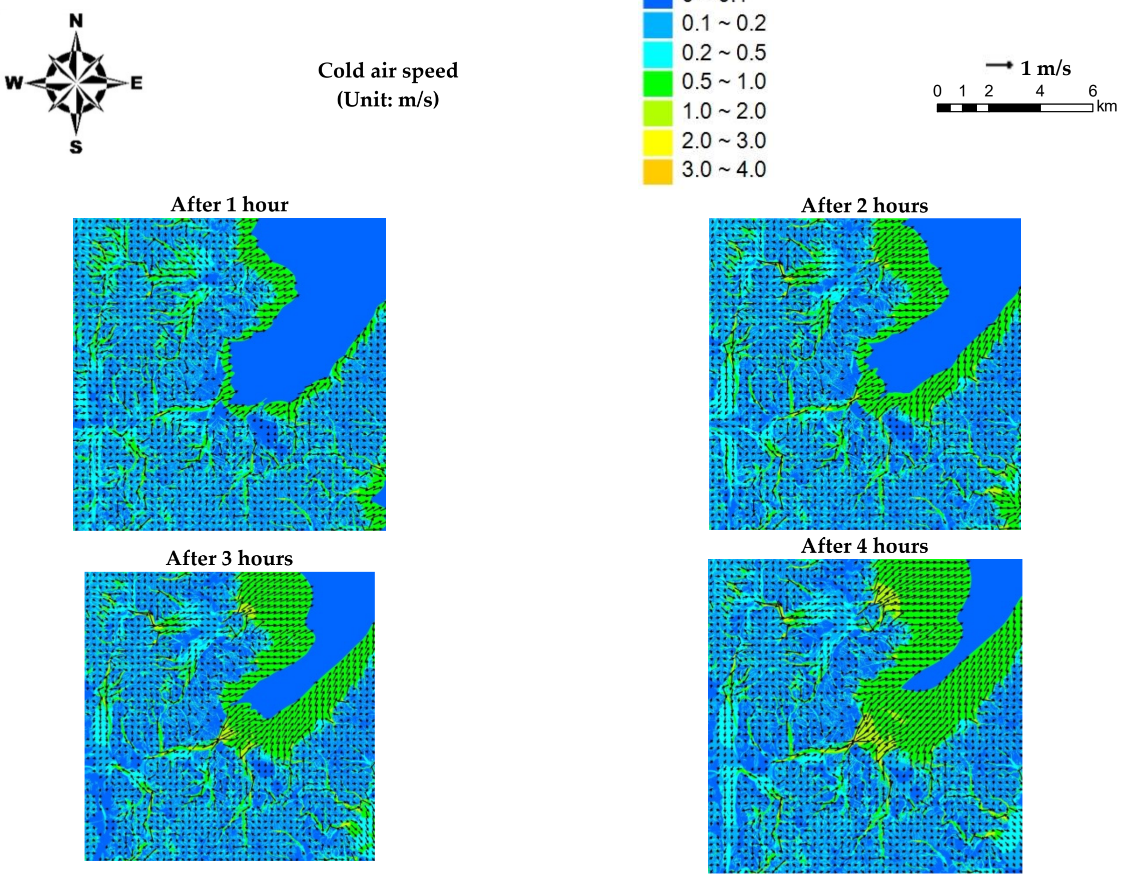

Figure 4. *Cont.*

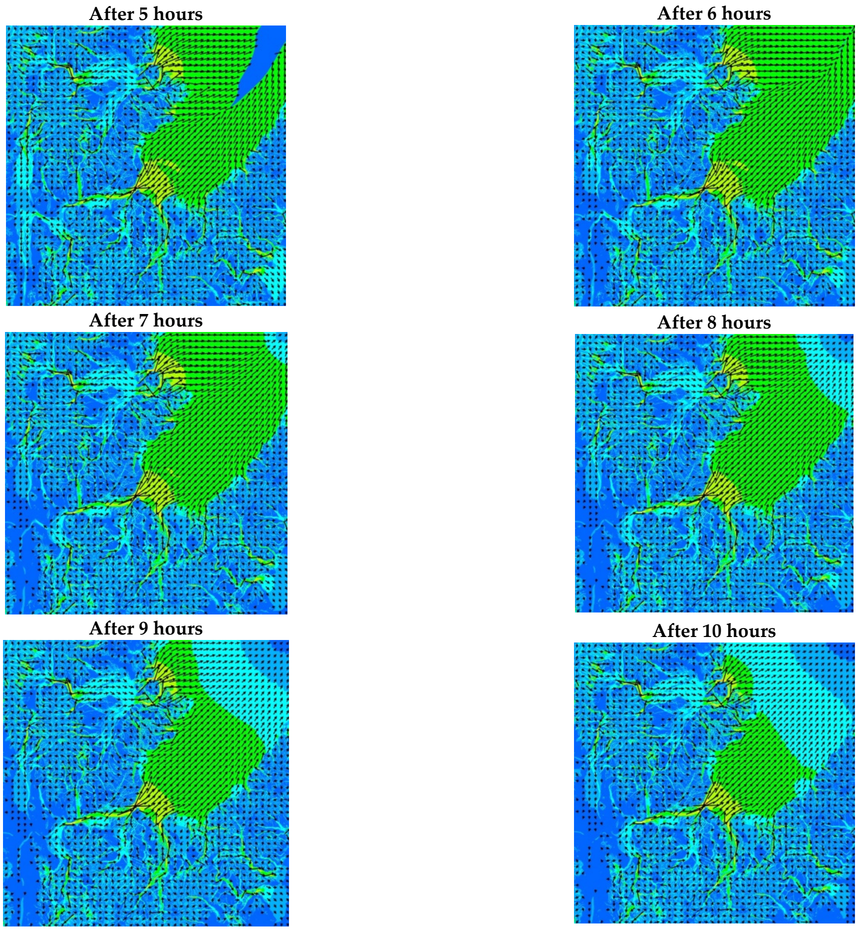

Figure 4. Graphical representation of the speed and flow direction of cold air in the study area (after 1–10 h).

3.1.2. Simulation of Cold Air Height and Flow Direction

To analyze the general wind environment of the study area, the height and flow direction of cold air generated in the study area were modeled per hour for a 10 h period. After 1 h (approximately 21:00), the cold air generated by nearby mountains flowed into the valley's base following the terrain's spatial characteristics; the cold air accumulated in the valley. In certain areas near the valley's base, cold air accumulated at a height of 30 m. After 2 h (approximately 22:00 h), the flow range of the cold height became even broader than that after 1 h. The flow range of cold air expanded along the stream (Hyeongsan River) and flowed into low-lying areas. After 3 h (approximately 23:00), the flow range and amount of accumulated cold air increased further, and the cold air flowed along the Hyeongsan River, gradually flowing into the city (Hyogok-dong, Daei-dong, and Jukdo-dong). After 4 h (approximately 00:00 h), the range of cold air flowing along the stream (Hyeongsan River) expanded slowly, and the speed of cold air flowing into the city accelerated, where the areas with cold air accumulated above an elevation of 30 m expanded. Cold air flowing along the stream moved quickly toward the East Sea. After 5 h (01:00– 06:00), most parts of the city experienced the influence of cold air in areas where cold air accumulated above an elevation of 40 m. Cold air was actively generated and flowed in the early morning; therefore, most parts of the study area experienced the influence of cold air after 6 h. The simulation results for cold air height and flow range showed that the cold air generated after sunset flowed by the spatial characteristics of the terrain. Specifically, the cold airflow range expanded quickly along the stream (Hyeongsan River), which indicated that the stream was the major wind corridor in the region. The flow of cold air exhibited a similar pattern after the midpoint of the simulation, gradually expanding its range around the stream (Hyeongsan River). The analysis results of the cold air height and flow range in Pohang indicated that the cold air height and flow range expanded around the Hyeongsan River, and the city center (Daei-dong, Jukdo-dong, and Songdo-dong) was influenced by cold air after 5 h. Figure 5 shows a graphical representation of the results.

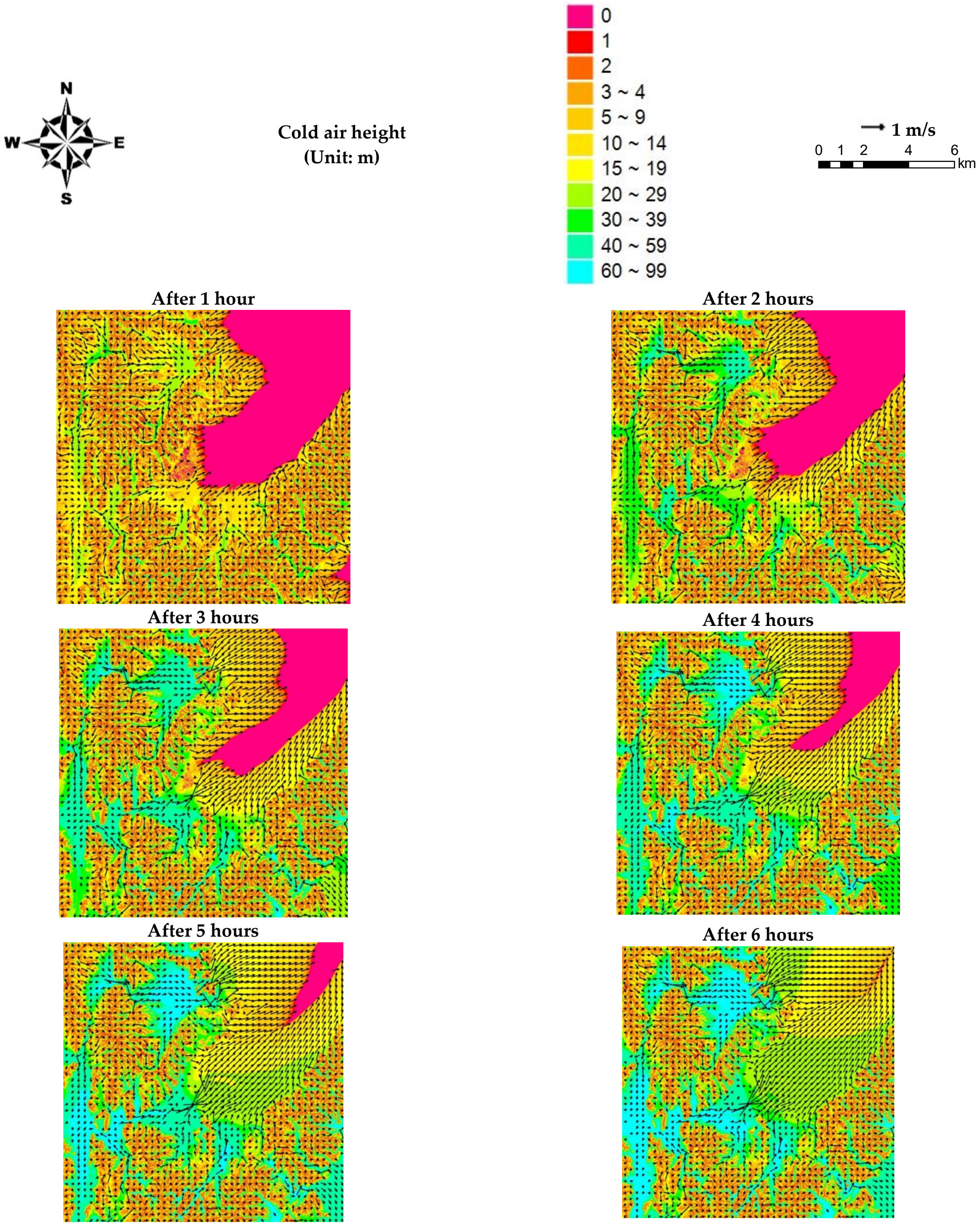

Figure 5. *Cont.*

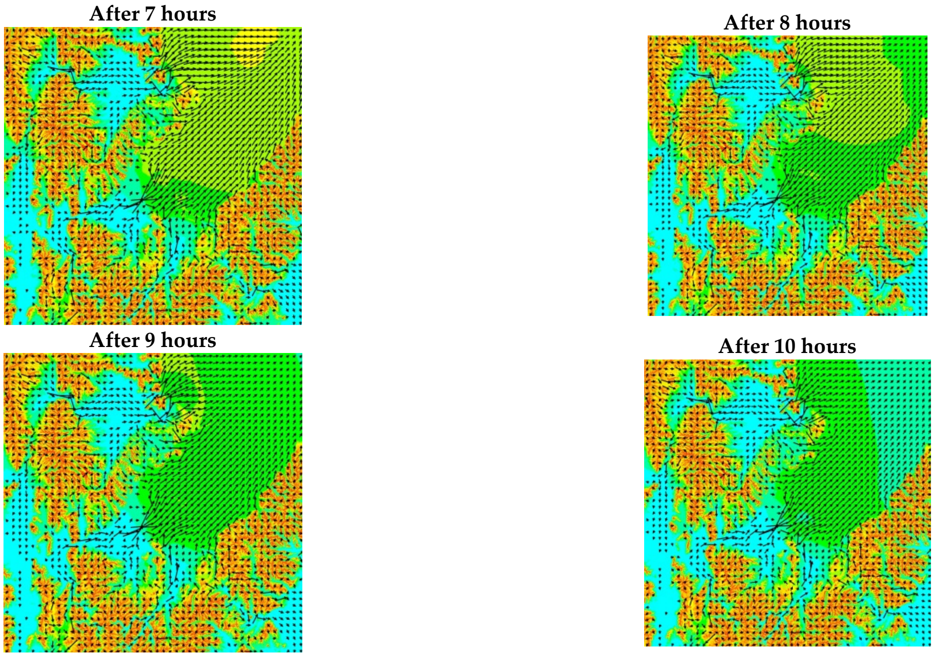

Figure 5. Graphical representation of the height and flow direction of cold air in the study area (after 1–10 h).

3.1.3. Simulation of the Changes in Cold Air Height

We analyzed the effects of using a water curtain (Hyeongsan Big Bridge, POSCO Bridge) to guide the flow of cold air, which was followed by the Hyeongsan River (a major wind corridor in Pohang City) toward the East Sea, circulating air to the surrounding areas. A simulation analysis was conducted to analyze the difference in cold air height before and after the water curtains were installed on the bridges (the POSCO and Hyeongsan Big bridges). The cold air height was quantitatively compared by the hour before and after the application of the water curtain. After 1 h, on the inner side of the bridge (Hyeongsan River) where the water curtain was installed, cold air accumulated 1 m to 9 m higher than observed before applying the water curtain. On the outer side of the bridge (East Sea), cold air accumulated at 1 m to 4 m lower compared to that observed before applying the scenario. After 2 h, this tendency became more apparent as the range of influence expanded to nearby towns. After 3 h, the cold air in the areas near the inner side of the bridge accumulated 10 m to 19 m higher than before applying the scenario, whereas the cold air in the areas near the outer side of the bridge was 10 m to 19 m lower than that observed before applying the scenario. After 4 h of applying the water curtains, the increasing trend in the cold air height on the inner side of the bridge expanded throughout the entire city, and the decreasing trend in the cold air height on the outer side of the bridge expanded over larger areas. Overall, operating the water curtains installed on the bridges guided the cold air flowing along the Hyeongsan River toward the East Sea to spread to nearby urban areas. Figure 6 shows a graphical representation of the results.

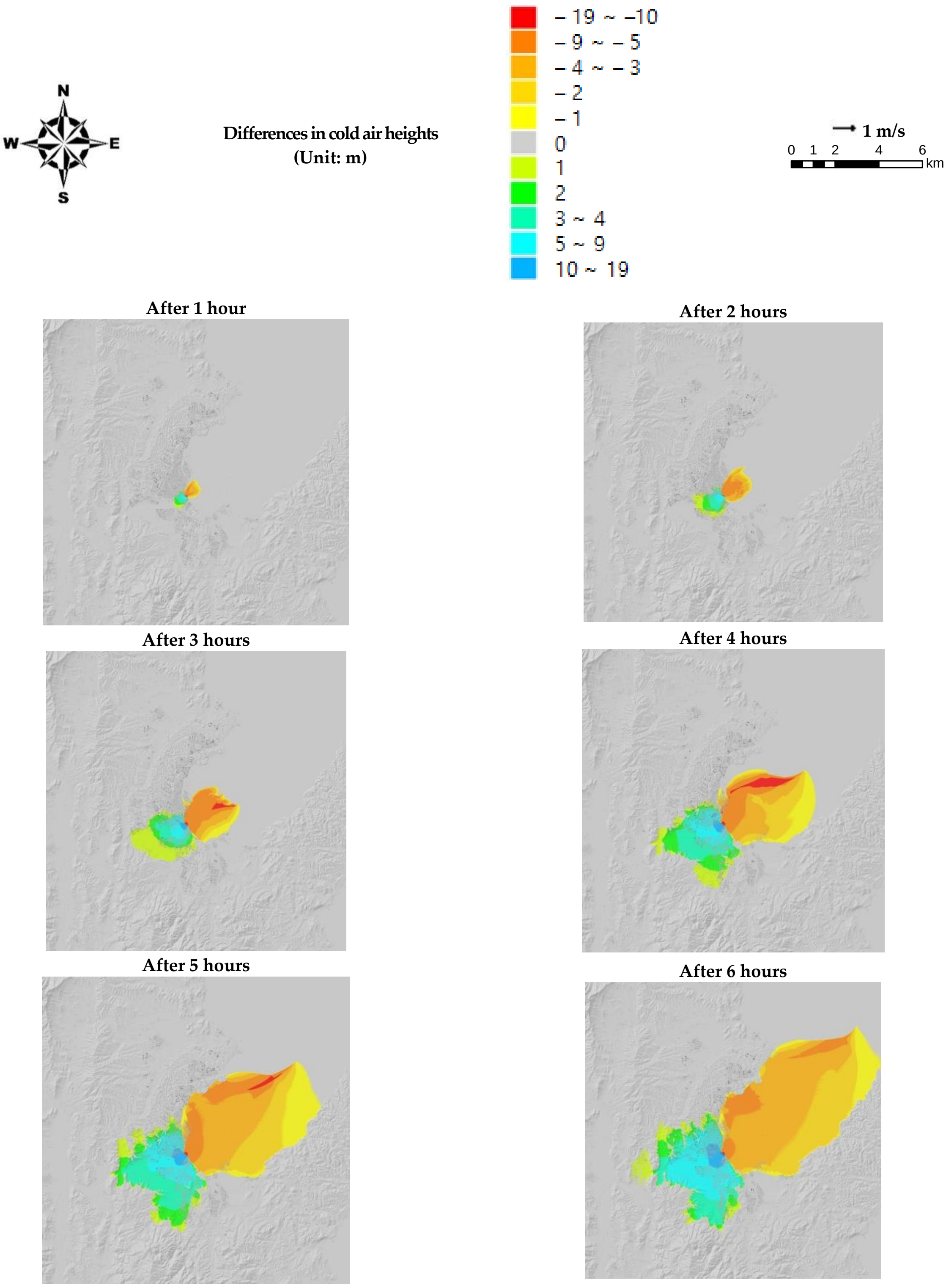

Figure 6. *Cont.*

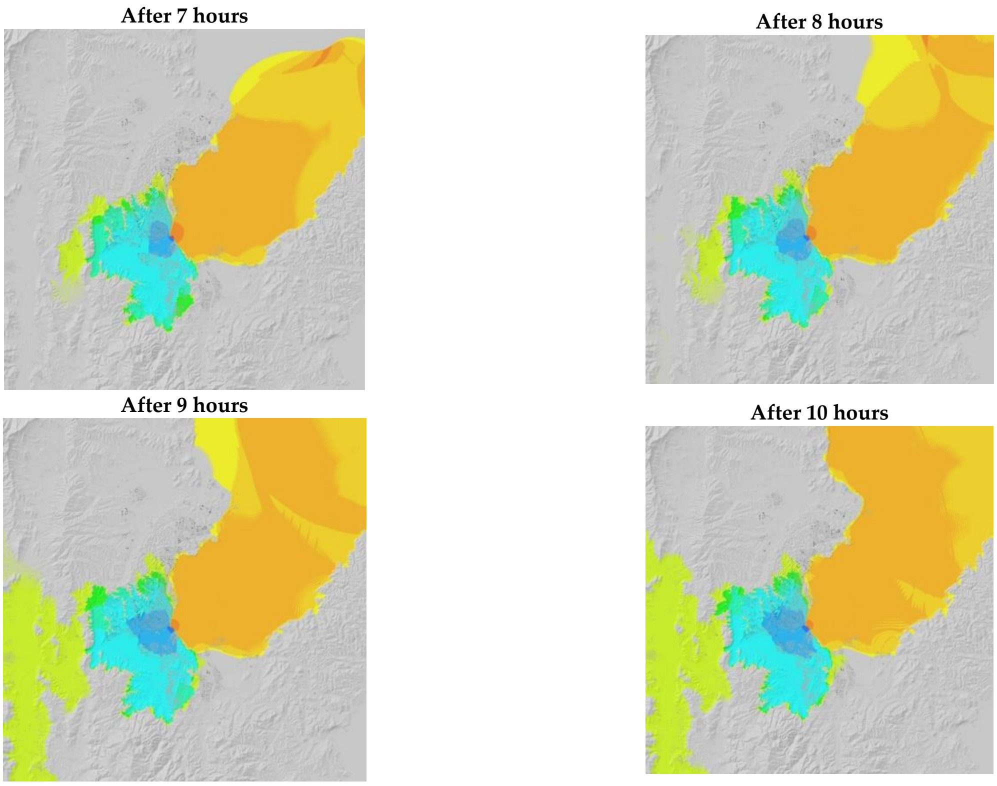

Figure 6. Comparison of the cold air heights in the study area with time after the application of the water curtains (after 1 h to 10 h).

Figure 7 shows the results of comparing the differences in the cold air heights of the study area 1 h to 10 h before and after applying the water curtains.

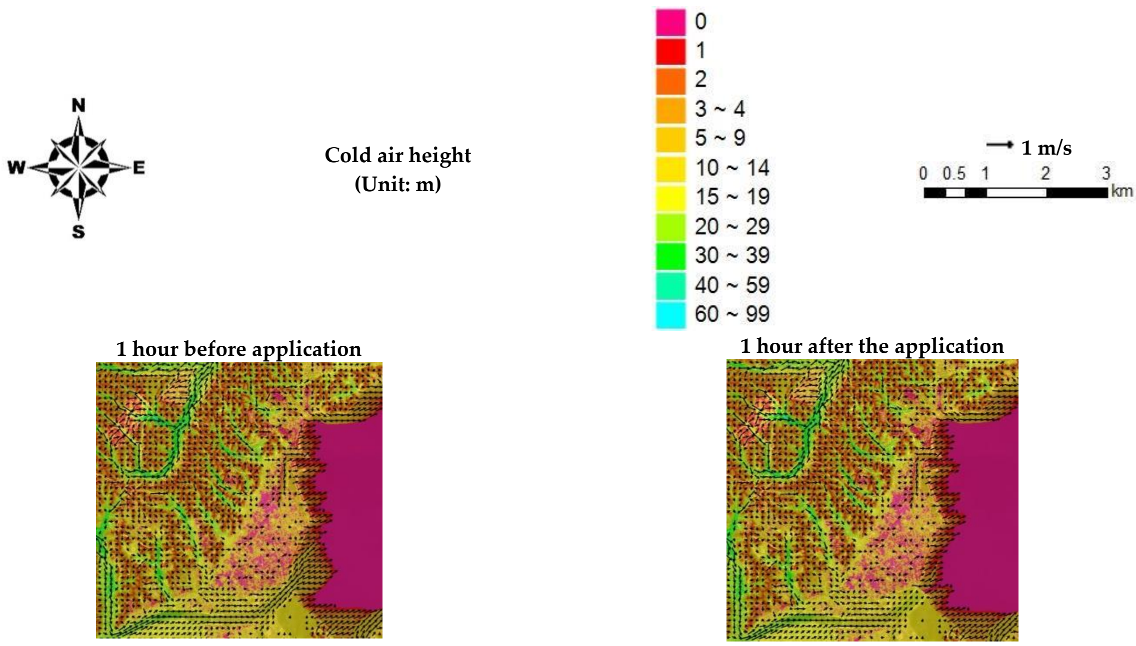

Figure 7. *Cont.*

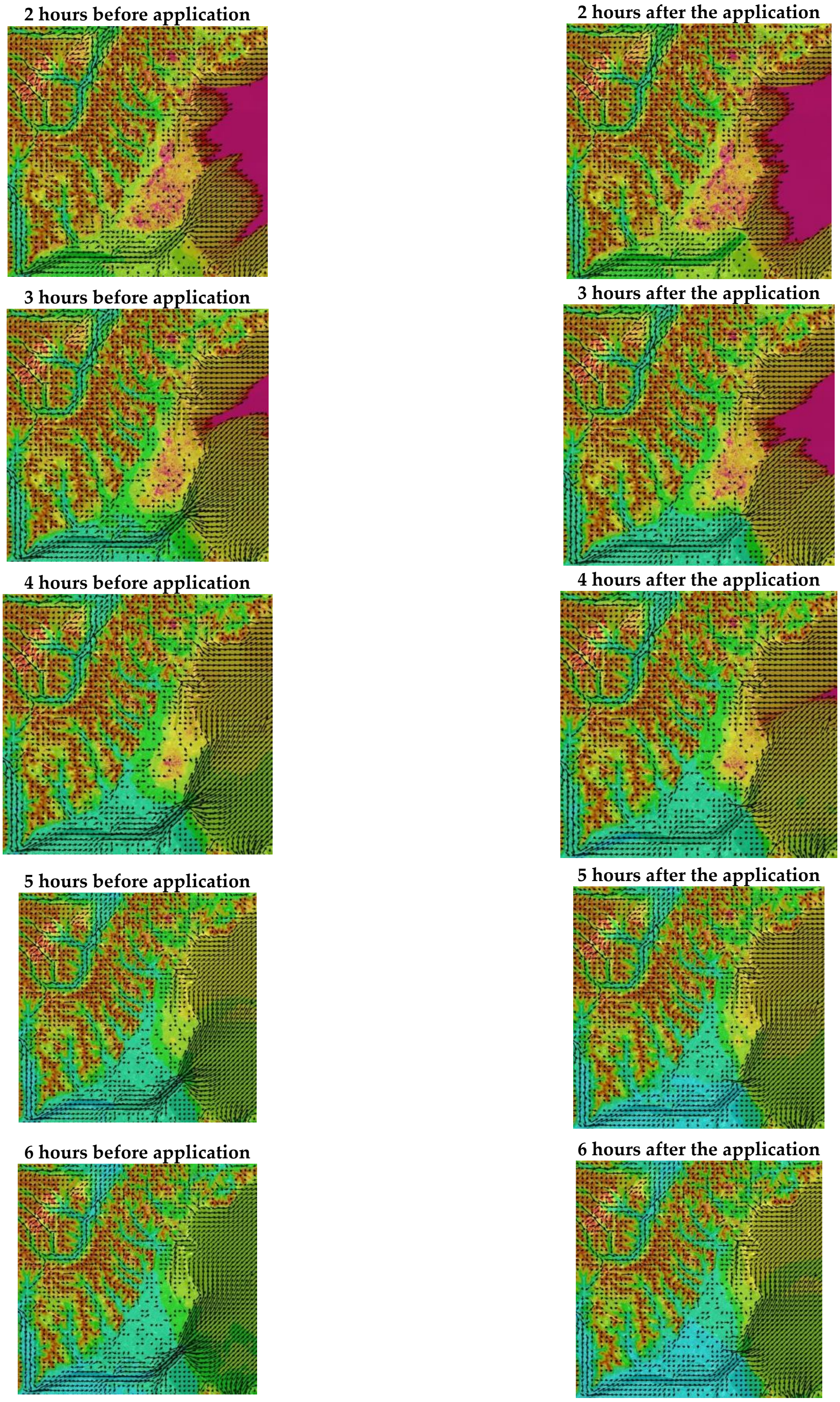

Figure 7. *Cont.*

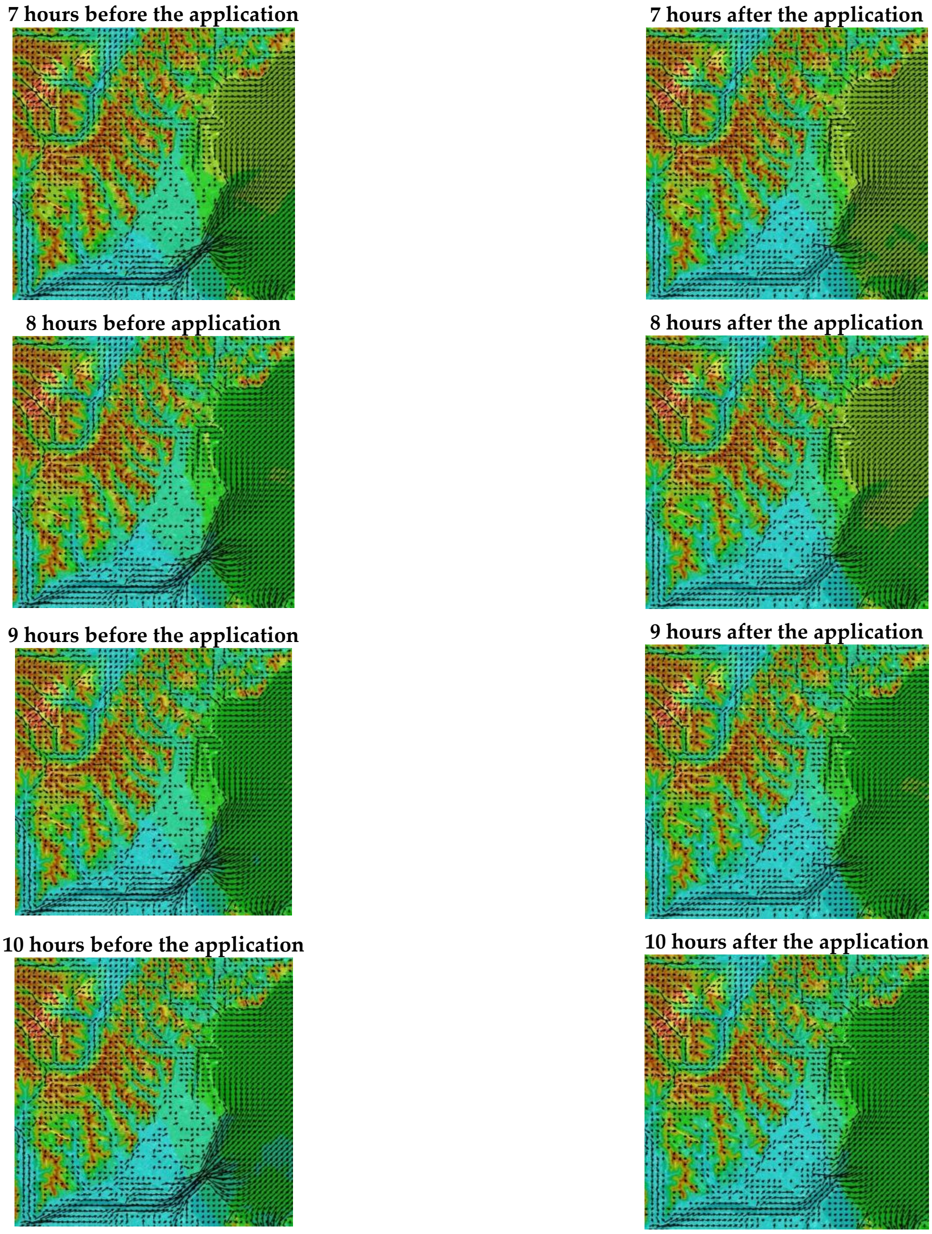

Figure 7. Extended comparisons of the differences in cold air heights in the study area 1–10 h before and after the application of water curtains.

3.2. Comparison of the Difference in Cold Air Heights at Major Observation Points

Three observation points were selected on the inner and outer sides of the water curtains, and the changes in the cold air heights were compared before and after applying the scenario. The three observation points on the inner side were as follows: (A) Pohang Nam-gu Office (X:1,167,571, Y:1,780,587), (B) Daedo Sageori (X:1,167,673, Y:1,781,700), and (C) Ogeori (X:1,168,120, Y:1,783,374). The three observation points on the outer side were (D) Pohang Inner Harbor Boat Dock (X:1,169,175, Y:1,782,384), (E) Pohang Meteorological Observatory (X:1,169,382, Y:1,783,319), and (F) East Sea (X:1,170,331, Y:1,783,743) (Figure 8). The coordinate values were based on the UTM-K (EPSG:5179) coordinate system.

Figure 8. Map portraying the observation points.

The address of point A is 790, Huimang-daero, Nam-gu, Pohang-si, Gyeongsangbuk-do.

Table 2 and Figure 9 showcase a comprehensive analysis of changes in cold air height over time. Two distinct trends are evident: the cold air height before the scenario application consistently trails the height observed after the scenario's implementation. Notably, there is a gradual increase in the difference between these two conditions over time, starting from 0.0 m at the 1 h mark and expanding to a 13.2 m difference by the 10 h mark. This suggests a significant impact of the scenario on the height of cold air over time.

Table 2. Comparison of the changes in the cold air heights at point A (Pohang Nam-gu Office).

Time Elapsed (h)	Cold Air Height (m)		
	Before Applying the Scenario	After Applying the Scenario	Difference
After 1 h	13.3	13.3	0.0
After 2 h	21.6	24.8	+3.2
After 3 h	37.3	42.7	+5.4
After 4 h	46.0	53.5	+7.5
After 5 h	51.6	60.7	+9.1
After 6 h	55.5	65.9	+10.4
After 7 h	58.7	69.9	+11.2
After 8 h	61.3	73.3	+12.0
After 9 h	63.5	76.2	+12.7
After 10 h	65.4	78.6	+13.2

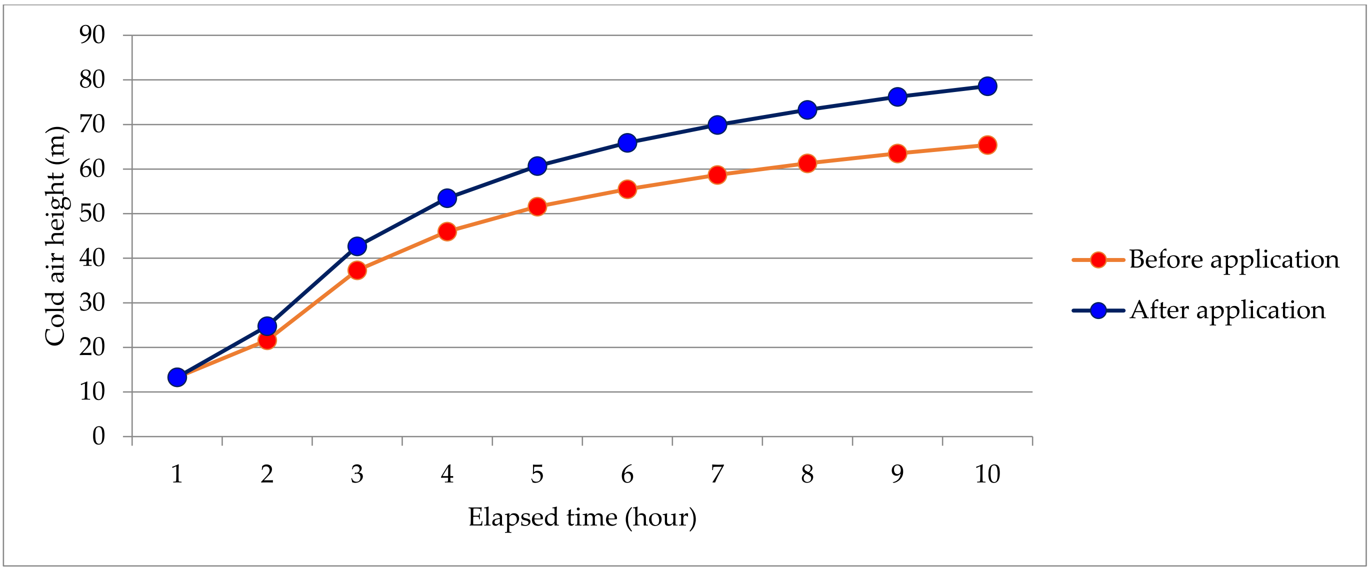

Figure 9. Comparison of the changes in the cold air heights at point A (Pohang Nam-gu Office) before and after the application of water curtains.

As shown in Table 3 and Figure 10, there is a substantial increase in cold air height following the application of water curtains, with an 11.4 m disparity observed at the ten-hour mark.

Table 3. Comparison of the changes in the cold air heights at point B (Daedo Sageori).

Time Elapsed (h)	Cold Air Height (m)		
	Before Applying the Water Curtains	After Applying the Water Curtains	Difference
After 1 h	4.6	4.6	0.0
After 2 h	8.1	8.9	+0.8
After 3 h	16.6	20.3	+3.7
After 4 h	34.4	41.8	+7.4
After 5 h	44.5	53.0	+8.5
After 6 h	50.2	60.6	+10.4
After 7 h	54.1	65.0	+10.9
After 8 h	57.4	68.4	+11.0
After 9 h	60.2	71.1	+10.9
After 10 h	62.1	73.5	+11.4

At point C, from 1 h to 4 h, there is no observable difference in cold air height, with both conditions showing identical values (Table 4 and Figure 11). However, starting from the fifth hour, a distinct increase in cold air height is noted in the scenario where water curtains are applied, with the difference gradually widening over time, reaching a peak difference of 6.1 m at the tenth hour.

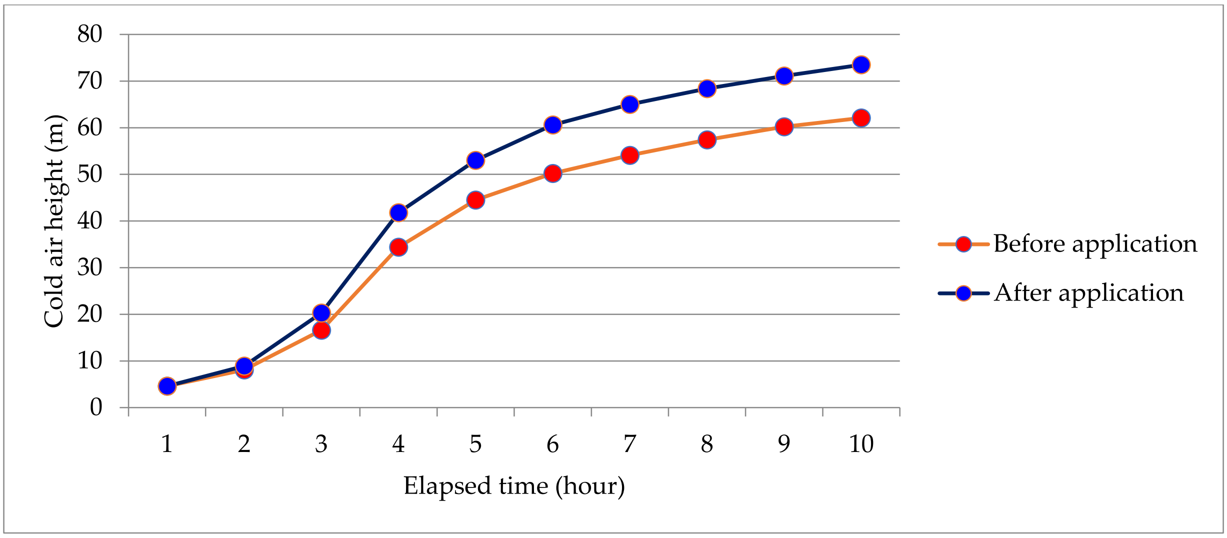

Figure 10. Comparison of the changes in the cold air heights at point B (Daedo Sageori) before and after the application of water curtains.

Table 4. Comparison of the changes in the cold air heights at point C (Ogeori).

Time Elapsed (h)	Cold Air Height (m)		
	Before Applying Water Curtains	**After Applying Water Curtains**	**Difference**
After 1 h	2.1	2.1	0.0
After 2 h	5.8	5.8	0.0
After 3 h	13.3	13.3	0.0
After 4 h	22.8	22.8	0.0
After 5 h	30.1	31.9	+1.8
After 6 h	37.4	41.1	+3.7
After 7 h	41.9	46.6	+4.7
After 8 h	44.8	50.2	+5.4
After 9 h	47.2	53.0	+5.8
After 10 h	49.3	55.4	+6.1

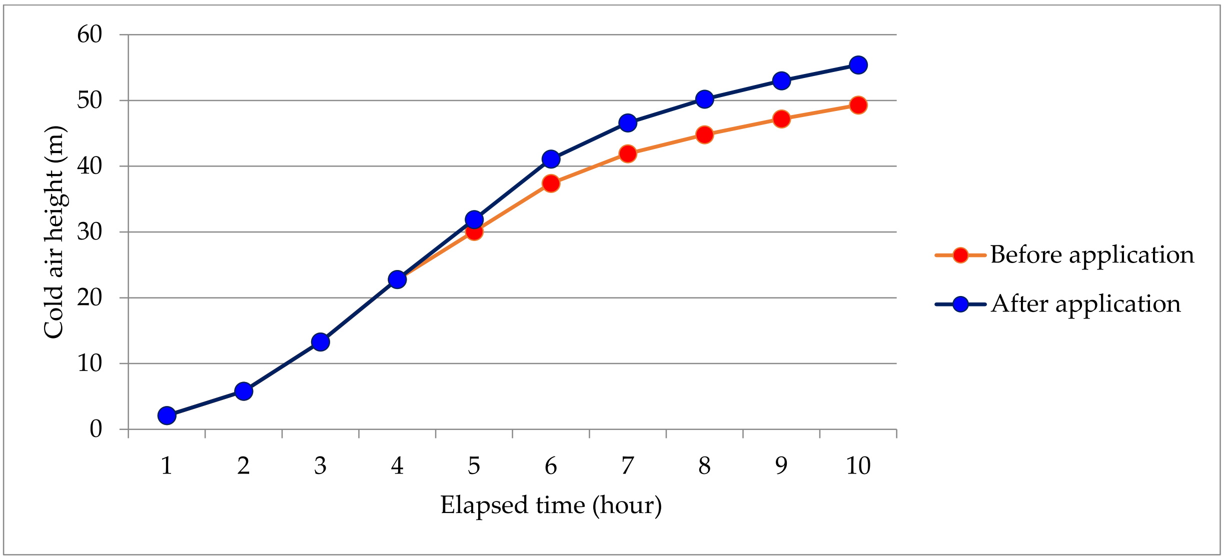

Figure 11. Comparison of the changes in the cold air heights at point C (Ogeori) before and after the application of water curtains.

The observations on the outer side have contrasting results. At point D, before the application of water curtains, the cold air height steadily increased over time, as indicated by Table 5 and Figure 12. However, after the application of water curtains, the cold air height shows a different trend, which is consistently lower than without water curtains, reaching a difference of —3.2 m at the tenth hour.

Table 5. Comparison of the changes in the cold air heights at point D (Pohang Inner Harbor Boat Dock).

Time Elapsed (h)	Cold Air Height (m)		
	Before Applying Water Curtains	After Applying Water Curtains	Difference
After 1 h	2.3	2.3	0.0
After 2 h	7.5	2.5	−5.0
After 3 h	16.0	8.8	−7.2
After 4 h	22.4	15.8	−6.6
After 5 h	27.1	21.4	−5.7
After 6 h	30.8	26.2	−4.6
After 7 h	33.8	29.5	−4.3
After 8 h	36.4	32.6	−3.8
After 9 h	38.8	35.3	−3.5
After 10 h	40.9	37.7	−3.2

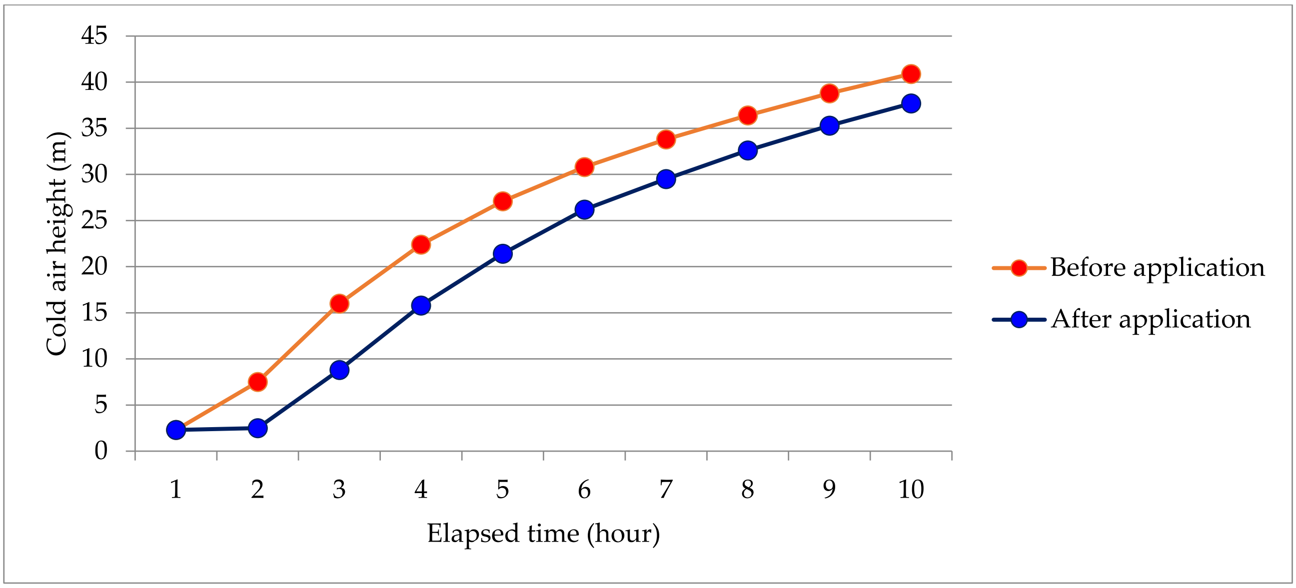

Figure 12. Comparison of the changes in the cold air heights at point D (Pohang Inner Harbor Boat Dock) before and after the application of water curtains.

At point E, at the 1 h mark, both situations indicate an equal cold air height of 7.4 m. As time progresses to the 2 h mark, both scenarios still show an identical height of 8.2 m, maintaining parity. However, from the 3 h point onward, a noticeable difference begins to emerge, with the post-scenario line consistently registering lower cold air heights compared to the pre-scenario conditions. The most significant differences are observed after the 4 h mark, where the cold air height in the post-scenario condition is 5.6 m lower than its pre-scenario counterpart, and this gap continues, with the difference slightly decreasing over time but remaining substantial until the end of the observed period (Table 6 and Figure 13).

Table 6. Comparison of the changes in the cold air heights at point E (Pohang Meteorological Observatory).

Time Elapsed (h)	Cold Air Height (m)		
	Before Applying the Scenario	After Applying the Scenario	Difference
After 1 h	7.4	7.4	0.0
After 2 h	8.2	8.2	0.0
After 3 h	10.1	8.4	−1.7
After 4 h	16.1	10.5	−5.6
After 5 h	21.2	16.2	−5.0
After 6 h	25.3	21.1	−4.2
After 7 h	29.1	25.1	−4.0
After 8 h	32.2	28.8	−3.4
After 9 h	34.9	31.9	−3.0
After 10 h	37.4	34.6	−2.8

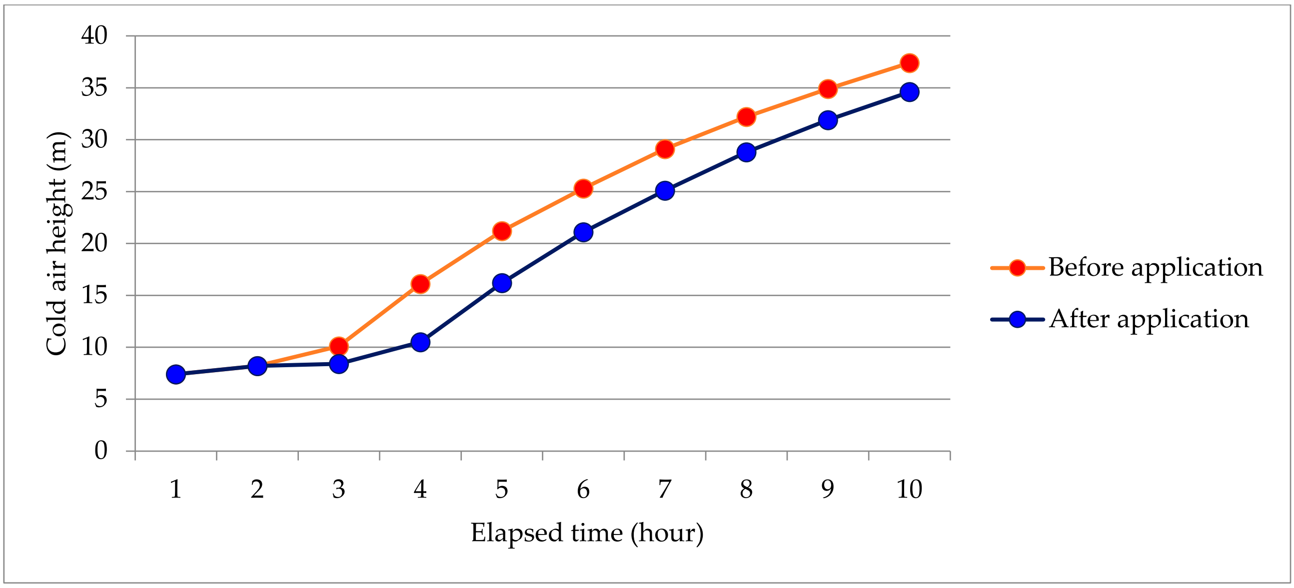

Figure 13. Comparison of the changes in the cold air heights at point E (Pohang Meteorological Observatory) before and after the application of water curtains.

At point F, for the first 2 h, there is no observable change in the height of cold air, indicating zero effect from the water curtains. However, as time progresses, a noticeable divergence appears from the third hour onwards, where the cold air height begins to increase significantly in the scenario without water curtains, while a much more gradual increase is observed when water curtains are applied. Without water curtains, the cold air height reaches 38.3 m after 10 h, whereas, with water curtains, the height is limited to 35.5 m, indicating a mitigating effect on the rise of cold air (Table 7 and Figure 14).

The cold air heights at the major observation points exhibited significant differences 2 h to 3 h after water curtain application.

Table 7. Comparison of the changes in the cold air heights at point F (East Sea).

Time Elapsed (h)	Cold Air Height (m)		
	Before Applying Water Curtains	After Applying Water Curtains	Difference
After 1 h	0.0	0.0	0.0
After 2 h	0.0	0.0	0.0
After 3 h	8.6	0.5	−8.1
After 4 h	15.8	10.0	−5.8
After 5 h	20.9	16.2	−4.7
After 6 h	25.2	20.9	−4.3
After 7 h	29.4	25.3	−4.1
After 8 h	32.6	29.3	−3.3
After 9 h	35.6	32.5	−3.1
After 10 h	38.3	35.5	−2.8

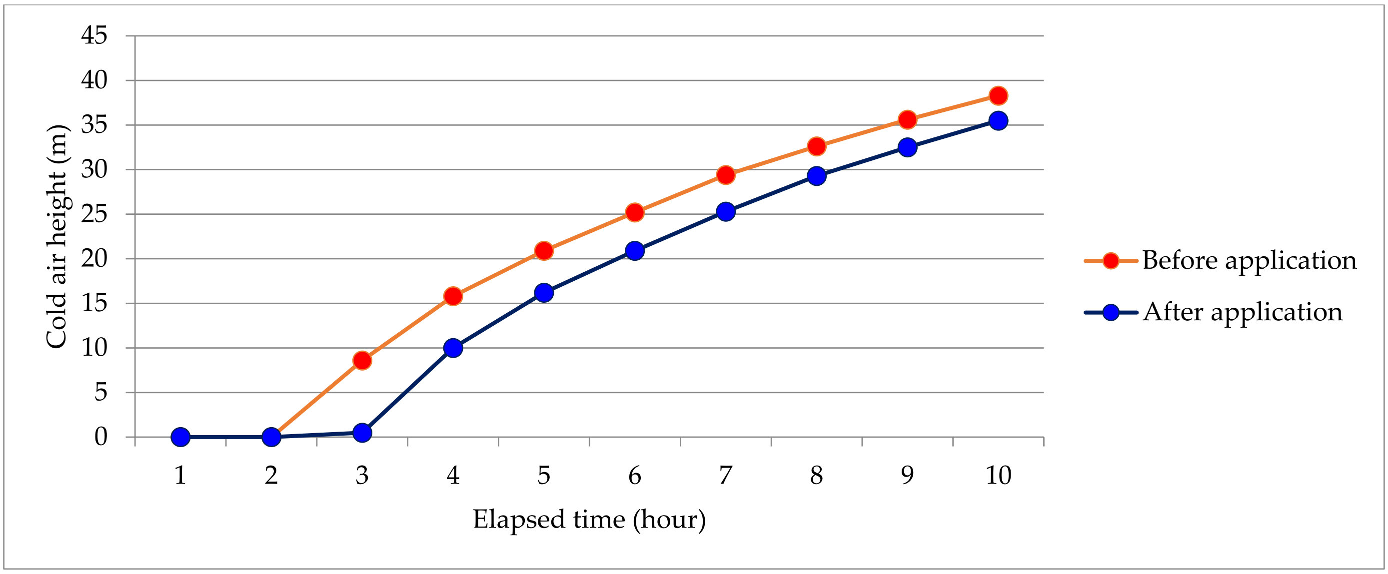

Figure 14. Comparison of the changes in the cold air heights at point F (East Sea) before and after the application of water curtains.

3.3. Analysis of Urban Wind-Corridor Forests

3.3.1. Wind-Generating Forests

"Wind-generating forests" refers to forests and green areas on the outskirts of a city, wherein cold air is generated at night and from where purified cold air blows. The total area of forests located inside and outside the city, corresponding to the wind-generating forest in the study area, was 374.9 km^2. The Unjesan, Sambongsan, Seongjeoksan, Johyangsan, and Doeumsan mountains are included in the area. Mountains surrounded the study area on three sides, and the forests consist of broad-leaved and coniferous trees, making them suitable for generating cold air. The side facing the ocean facilitated wind movement during the day and night. In addition, cold air generated from the forests could flow quickly along the Hyeongsan River and toward the city center (Figure 15).

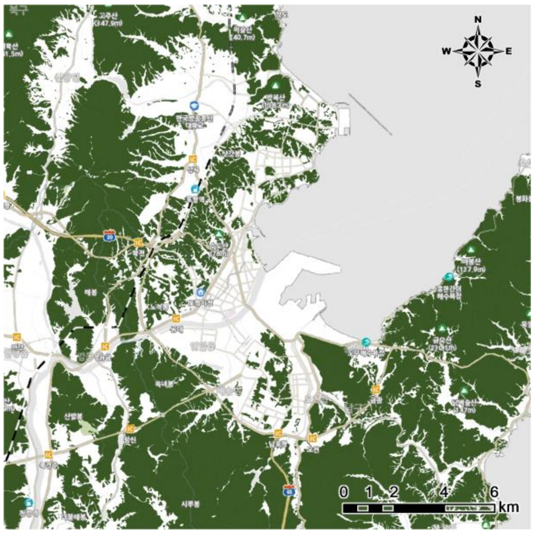

Figure 15. Map portraying the wind-generating forests in the study area.

3.3.2. Wind-Connecting Forests

A connecting forest refers to green lands that help the cold air generated in a wind-generating forest to flow into the city; it encompasses linear and belt greens, including roadside trees and riverbanks. The total area of green facility land inside the city corresponding to the connecting forests in the study area was 2.5 km^2. In total, 357 landscapes, buffers, and other green spaces were included in the study area. Roadside trees also belong to wind-connecting forests, but they were excluded because of limitations in collecting the relevant information space data. The study area was suitable as a wind-connecting forest through two local roads, five national roads, the Iksan-Pohang and Donghae expressways, and a plant-based ring road surrounding the city. In particular, a wind corridor of cold air formed along the 50 m wide Hyeongsan River and smaller streams, including the Naengcheon and Chilseongcheon streams (Figure 16).

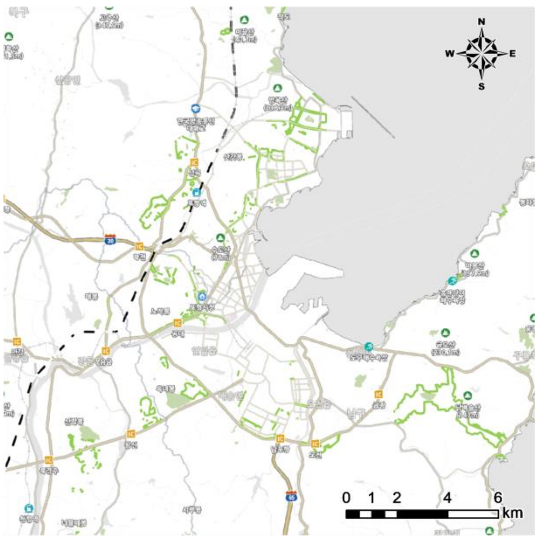

Figure 16. Map portraying the wind-connecting forests in the study area.

3.3.3. Wind-Spreading Forests

A wind-spreading forest refers to a base forest in a city that generates a breeze owing to the temperature difference between the city and forest areas. It includes diverse greening methods, such as parks, rooftop parks, and school forests, and utilizes techniques such as low-rise planting and green parking lots to optimize land use in densely developed urban areas without obstructing airflow. Strategically planting trees with wide canopies, along with grass cover, creates shade and promotes evapotranspiration for temperature regulation. In this study, the total area of wind-spreading forests within the study area located inside and outside the city was 0.5 km^2. The city included 174 children's, neighborhood, and small parks. It was divided into old and new towns, encompassing parks and school forests, while the Old Town consisted of relatively narrow urban spaces and clustered buildings, in addition to a low ratio of green land, and although trees and green spaces in residential areas might play an important role in wind transmission, small and fragmented areas make it unsuitable for wind-spreading forests (Figure 17).

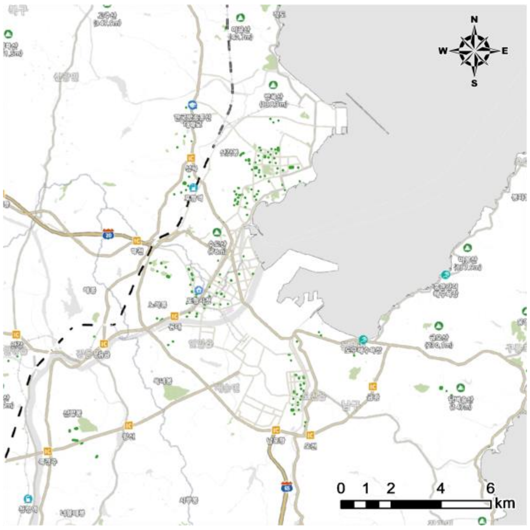

Figure 17. Map of wind-spreading forests in the study area.

3.3.4. Overall Status

Wind-generating forests account for most of the outskirts of the study area, whereas wind-connecting and wind-spreading forests are distributed throughout the inner part of the city. The study area is surrounded by mountains on three sides, cold air is generated in various vegetation forests, and wind can quickly move toward the ocean on one side. Furthermore, a connecting forest can be formed by a ring road surrounding the city, two expressways into the city, and five national and two local roads. Specifically, the cold air generated in the forests can quickly flow into the city center through the Hyeongsan River and the Naengcheon and Chilseongcheon streams. However, the Old Town has a higher population density than the New Town, with narrow urban spaces, clustered buildings, and a lower GAR; thus, the Old Town would not be suitable as a wind-spreading forest (Figure 18).

3.4. Correlation Analysis of Cold Air Speed and Green Area Ratio (GAR) of Urban Wind-Corridor Forest

3.4.1. Green Area Ratio (GAR) of Urban Wind-Corridor Forest by Grid

This study assessed the area ratio of urban wind-corridor forests per grid in the study area. Approximately 50% of the area had a 0% to 30% ratio of green coverage, and the number of grids increased gradually from 30% to 80% GAR and sharply increased to 224 (6.2%) at 80% to 90% GAR and 804 (22.3%) at 90% to 100% GAR (Table 8 and Figure 19).

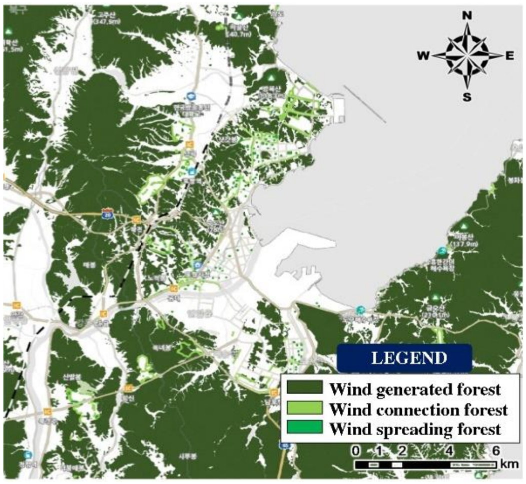

Figure 18. Map portraying urban wind-corridor forests in the study area.

Table 8. Green area ratios (GARs) of urban wind-corridor forest by grid (500 m × 500 m).

Category	0%	0–30%	30–40%	40–50%	50–60%	60–70%	70–80%	80–90%	90–100%
No. of grids	1203	551	143	164	166	172	173	224	804
Ratio (%)	33.4	15.3	4.0	4.6	4.6	4.8	4.8	6.2	22.3

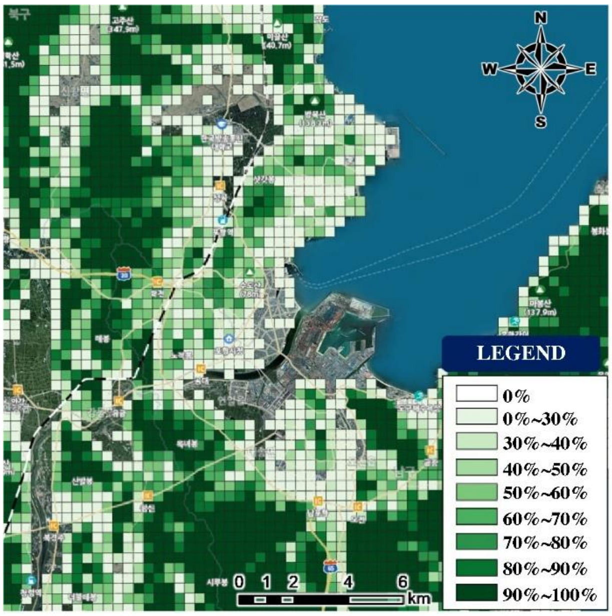

Figure 19. Map portraying the correlation between urban wind-corridor forests and green area ratio (GAR) by grid (500 m × 500 m).

3.4.2. Cold Air Speed by Grid

This study assessed the cold air speed of the study area per grid. The largest portion of 53% (1908 grids) of the total 3600 grids had flow speeds of 0.4–1 m/s, 22.3% (803 grids) had speeds of ≤0.4 m/s, 20% (719 grids) had speeds of 1–2 m/s, 4.1% (146 grids) had speeds of 2–3 m/s, and 0.6% (20 grids) had speeds of ≥3 m/s (Table 9).

Table 9. Cold air speed of urban wind-corridor forest by grid (500 m × 500 m).

Category	≤0.4 m/s	0.4–1 m/s	1–2 m/s	2–3 m/s	≥3 m/s
No. of grids	803	1912	719	146	20
Ratio (%)	22.3	53.1	20.0	4.1	0.6

3.4.3. Correlation Analysis

The Statistical Package for the Social Sciences (SPSS) program was used to perform a correlation analysis between cold airspeed and GAR. The Pearson correlation was measured after matching the GAR data by a grid with the cold airspeed; the GAR and cold air speed showed a positive correlation of +0.153 (Table 10, Figures 20 and 21).

Table 10. Correlation analysis results between green area ratio (GAR) and cold air speed.

		Green Area Ratio (GAR)	Cold Air Speed
Green area ratio	Pearson correlation	1	0.153 **
	Significance probability (both sides)		0.000
	N (total number of grids)	3600	3600
Cold air speed	Pearson correlation	0.153 **	1
	Significance probability (both sides)	0.000	
	N (total number of grids)	3600	3600

** $p < 0.01$.

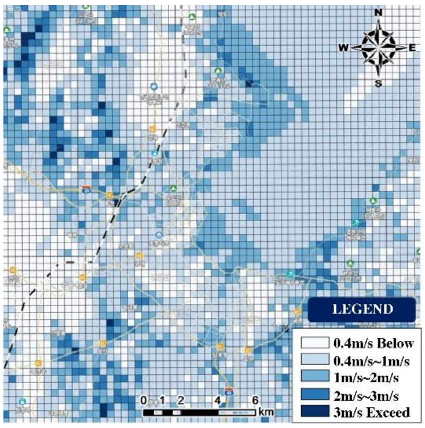

Figure 20. Map portraying the correlation between urban wind-corridor forests and cold air speed by grid (500 m × 500 m).

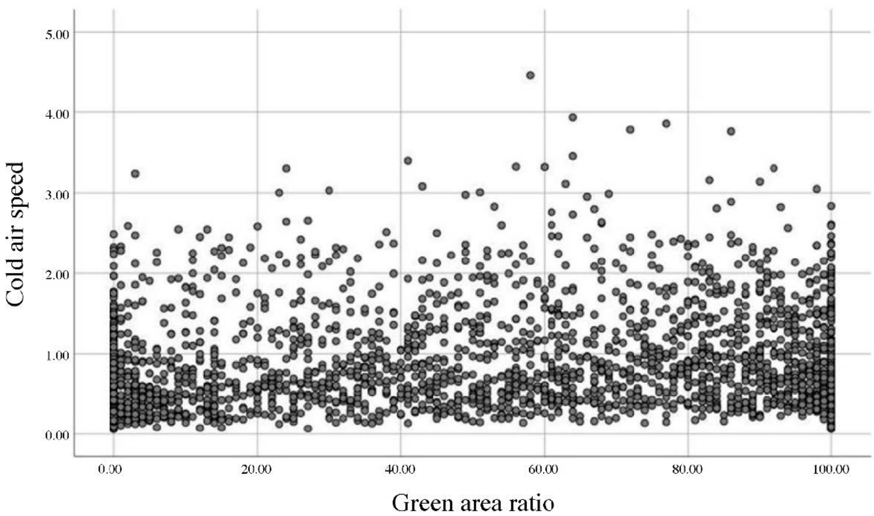

Figure 21. Scatter plot showing the correlation between cold air speed and green area ratio.

4. Wind Corridor Planning Strategy of Pohang

The following planning strategies are proposed based on an analysis of Pohang's cold airflow and wind-corridor forests. Considering the geographical location and type of wind corridor, the study area was divided into three regions. Region A was located in the Old Town with a fragmented wind-generating forest to the west, the POSCO bridge, and the ocean to the east. Thus, the air in the region tends to stagnate, and the city experiences fine dust and UHI phenomena. Based on cold air flow analysis, a water curtain was installed at the bridge in the Hyeongsan River to induce cold air to flow into the Old Town and diffuse stagnant air. The water curtain was operated at night to induce cold air to move toward the ocean and flow into the Old Town, and various greening technologies could be applied at the Hyeongsan River to form green areas around the riversides and embankments. In Region B, a low wind-generating forest was located to the west of the residential area, whereas the ocean was located to the east, northeast, and southeast. Low-type wind-generating, wind-connecting, and wind-spreading forests surrounded the residential area but were fragmented. Thus, plants in wind-generating and wind-connecting forests must be supplemented to improve the efficiency of wind corridors in guiding cold air into residential areas. The flow of cold air from the west had to be induced, which was considered the primary aim. Region C was surrounded by forests on three sides, except for the north (the POSCO Bridge was located to the north). Region C was the most suitable area for wind-generation forests. Furthermore, the city center in Region C was less crowded than in other regions, demonstrating a faster flow of cold air through a more dispersed area. Installing a water screen at the bridge in the Hyeongsan River north of Region C can induce the movement of cold air at night in Region A (Figures 22 and 23).

We propose four strategies for planning a smooth wind corridor in Pohang City based on an analysis of the cold airflow in the region. First, the wind-generating forest on the three sides surrounding the city must maximize the production capability of cold air; this can be achieved by thinning the forests and managing the forest structures and changes in vegetation. The vegetation index should be enhanced to create an environment that enables the stable growth of vegetation, and the density and height of the base of the wind-generating forest should be decreased to ensure that the generated cold air can flow smoothly through the region, as emphasized by Z. Wang et al. (2022b), who showed that a sparser arrangement of trees provides a more effective cooling effect compared to a denser planting pattern [26]. The climate and soil of the study area must be analyzed, and tree species appropriate for the region must be selected and planted to create a forest. The damaged forests should be restored and supplemented to enhance the vegetation index of the region. Improved air quality due to increased circulation of fresh, cold air can reduce respiratory issues and allergies among residents. Cold air can also alleviate heat-related illnesses during hot weather, promoting overall respiratory health and comfort [27]. Second, it is necessary to connect the wind flow using green areas along rivers and riverbanks to develop wind-connected forests. A study conducted by Jiang et al. (2018b) showed that vegetated water bodies had a large microclimate impact that improved the thermal environment in surrounding areas [28]. For various road types, ensuring that the surrounding land is designed to facilitate wind corridors is crucial. Building structures need to be improved while simultaneously promoting greening. Roadside trees must be planted efficiently to enhance wind flow while considering certain road condition factors, such as the width of roads and sidewalks. Altunkasa and Uslu (2020) propose the planting of deciduous trees in courtyards and pedestrian areas to offer shade in summer and allow sunlight penetration in winter. They also recommend the use of evergreen trees to the north of buildings to shield against winter winds in Adana, Turkey [29]. Old or weak roadside trees with low vegetation index should be replaced, and underplanting needs to be replaced entirely to prevent the road surface temperature from abruptly increasing during the day. Additionally, water may be sprayed on roads to prevent the rise of surface temperature and reduce fine dust. The streams' cold air generation effect can be further improved if the riverside surface is developed into grassland and trees are planted on the banks. The increased presence of greenery can have psychological benefits, reducing stress and improving mental well-being [30]. Third, for wind-spreading forests, existing parks must be improved while establishing new green zones that supplement areas with relatively weak cold airflow. The vegetation in existing urban parks can improve the effects of accumulated cold air while ensuring its diffusion. In addition, green areas should be expanded to include existing public institutions, schools, and private buildings. For instance, in the Glasgow Clyde Valley Region, the United Kingdom, increasing the existing green coverage ratio by 20% could potentially diminish the projected UHI effect by at least one-third by 2050 [31]. Larger areas with relevant functions for each zone must be secured through various green practices, such as building green parking lots and artificial ground greening, including fence demolition and rooftop and wall greening. Accessible green spaces provide opportunities for physical activity and outdoor recreation, which are essential for maintaining a healthy lifestyle. Increased green space availability is associated with lower rates of obesity, heart disease, and mental health disorders [32]. Notably, the coverage of artificial ground made of concrete must be minimized, and the land coverage of lawns and natural grasslands must be maintained to secure the production, storage, and diffusion of cold air. Finally, impermeable road pavements should be replaced with permeable pavements. Fourth, to resolve the routine UHI phenomenon and alleviate fine dust pollution in the Old Town, water curtains can be installed on the bridges in the Hyeongsan River to guide cold air into the city center, thus effectively diffusing stagnant air into the city. Water curtain systems offer versatile design options and control mechanisms, making them potential solutions for urban planning and street landscaping interventions focused on improving outdoor comfort and reducing the UHI effect. With minimal installation, operation, and maintenance costs, these systems provide an affordable solution for enhancing the environmental quality of urban spaces [33]. They consume small amounts of water and do not require specialized hydraulic infrastructure, increasing their implementation feasibility in various settings. They can also contribute to expelling dust and pollutants from the surrounding area, promoting cleaner air and healthier environments, and preventing heat stress by providing emergency treatment for heat stroke [34]. Furthermore, the use of water curtains should be restricted during the daytime, and they should mainly be employed at night to induce the movement of cold air toward the sea and into the Old Town. Green spaces can be developed along the riversides and levees of the Hyeongsan River near the Old Town to facilitate a wind corridor to assist this process.

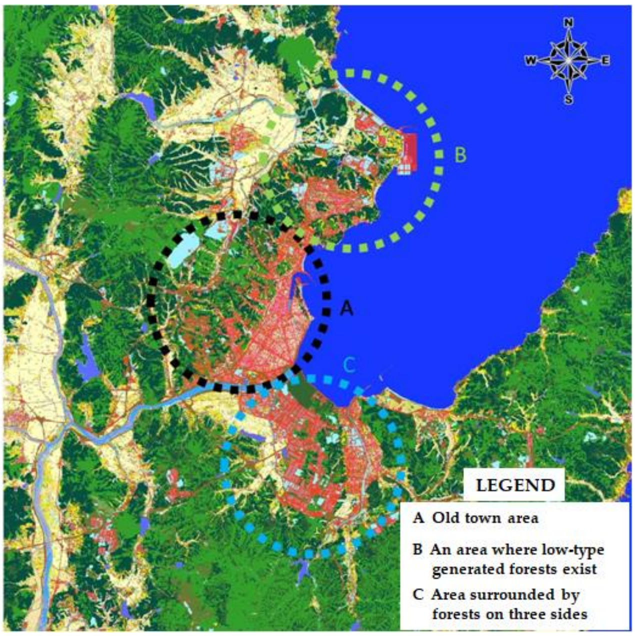

Figure 22. Map portraying the wind-corridor forest area division based on urban areas.

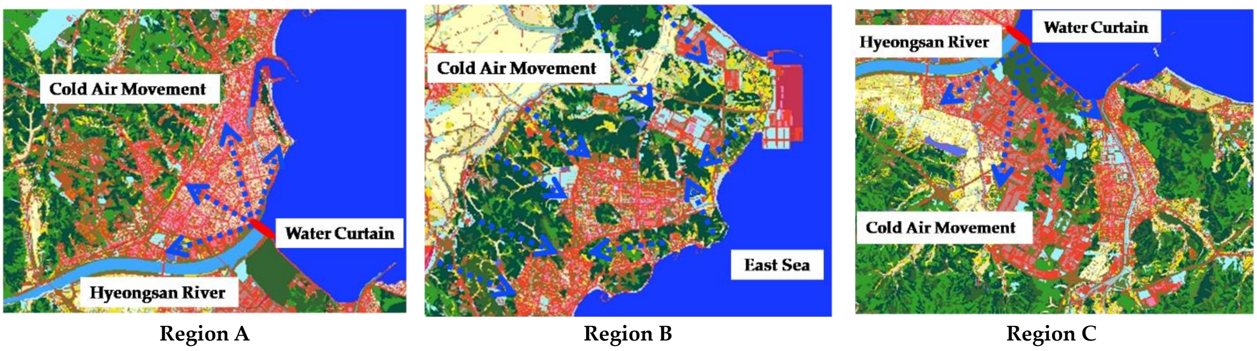

Figure 23. Maps portraying cold air movement division in Regions A, B, and C, based on urban areas.

5. Discussion

In this study, we examined measures that can reduce fine dust and alleviate the urban heat island (UHI) effect in Pohang City by analyzing the cold airflow. Notably, Pohang is severely affected by the urban heat island (UHI) effect. Therefore, this study highlights the importance of enhancing the thermal environment in Pohang and proposes a practical planning strategy for reducing the UHI effect by analyzing the flow of cold air in the region.

First, the demographic and social environment analyses indicated that the study area was an urbanized dry area of residential, commercial, and business areas surrounded by broad-leaved and coniferous forests on the city's outskirts. Regarding transportation and buildings, the Iksan-Pohang and Donghae expressways are located close to the national roads No. 7, 14, 20, 28, and 31, and local roads No. 929 and 945 pass through the city. Several buildings are densely located in the city center. This urban land configuration can significantly impact wind corridors by interfering with natural wind patterns, reducing green spaces, increasing surface roughness, and obstructing natural airflow. Buildings, roads, and other infrastructures can disrupt airflow patterns, decreasing ventilation and increasing the UHI effect. Loss of green spaces diminishes the formation and maintenance of wind corridors, while increased surface roughness disrupts smooth airflow. Changes in land use and obstruction of natural airflows further exacerbate these effects, resulting in stagnant air pockets and localized pollution buildup. Evidence-informed urban planning and design strategies are crucial to mitigate these impacts and promote healthier urban environments.

We considered meteorological observatories 1 ASOS 1 and 1 AWS to analyze the climatic environment characteristics. Pohang (138) is located at 70, Songdo-ro, Nam-gu, Pohang-si, and Gyeongsangbuk-do, whereas Guryongpo (816) is located at San4, Byeongpo-ri, Guryongpo-eup, Nam-gu, Pohang-si, and Gyeongsangbuk-do. Considering the representativeness of the observations at the Pohang Observatory (138), the monthly average wind speed over the past 10 years (2013–2022) was 2.67 m/s; notably, the speed has increased gradually. The most frequently observed wind flow direction by year was southwest, and the predominant wind direction over the past 10 years (2013–2022) was west–southwest (247.5°). A wind rose plot for 2013–2022 indicates that the predominant wind direction [west–southwest wind (227.5°)] had the highest frequency (21.7%), followed by southwest (19.1%), northeast (9.4%), and no (1.5%) wind.

Second, to analyze the general wind environment of the study area, the speed and flow direction of the cold air generated in the study area were modeled per hour for a 10 h period. The results indicate that after 1 h (approximately 21:00), the cold air generated from the surrounding mountains flowed toward the base of the valley (corresponding to the spatial characteristics of the terrain), and the cold air speed also increased gradually. The cold air speed was $\leq$0.2 m/s in most regions but reached up to 0.5 m/s in slopes, streams (Hyeongsan River), and main roads. After 2 h (around 22:00 h), the cold airspeed increased, especially at points where a valley began or along a stream (Hyeongsan River); the cold air speed was $\geq$1 m/s. After 3 h (approximately 23:00 h), the cold air speed increased consistently in most regions. In particular, the cold air speed increased further downstream of the Hyeongsan River (≥3 m/s), and the cold air quickly flowed along the stream and traveled toward the East Sea. After 4 h (approximately 24:00), cold air flowed consistently along the stream (Hyeongsan River), partially affecting the city. The cold air speed was ≤0.2 m/s in most parts of the city, while the speeds near the roads were 0.2–0.5 m/s. After 5 h (01:00–06:00), the cold airspeed gradually decreased as the simulation time elapsed. In contrast, cold air consistently and quickly flowed along the stream (Hyeongsan River), indicating that the river passing through Pohang was the major wind-corridor region. The simulation results of the cold air speed and flow direction showed that the cold air generated near the mountains (Doeumsan and Unjesan Mountains) after sunset moved quickly along the valley and stream and circulated with the air in the city. During the early hours of the simulation, the cold air speed generally decreased, except in the areas near the stream (Hyeongsan River); however, the inflow of cold air mostly continued around the stream, which implied that the stream was the major wind-corridor region of Pohang. The physical properties of cold air mean that it tends to flow from a higher elevation to a lower elevation (owing to its higher density than hot air), accumulates in the lower ground near the stream, and covers a wider range of area.

In the simulation of the cold air height and flow direction, after 1 h (approximately 21:00 h), the cold air generated from nearby mountains flowed into the valley's base following the spatial characteristics of the terrain where the cold air accumulates. Cold air accumulated at 30 m in certain areas near the valley's base. After 2 h (around 22:00 h), the range of cold height became even wider compared to that after 1 h. The flow range expanded beyond the valley along the stream (Hyeongsan River). Notably, cold air primarily flowed into the low-lying areas. After 3 h (around 23:00 h), the flow range and amount of accumulated cold air increased even further; in particular, the cold air flowed along the stream (Hyeongsan River) and moved slowly into the city (Hyogok-dong, Daei-dong, and Jukdo-dong). After 4 h (approximately 00:00 h), the range of cold air flowing along the stream (Hyeongsan River) gradually expanded, and the speed of cold air flowing into the city accelerated in areas where cold air accumulated above 30 m. Cold air flowing along the stream moved quickly toward the East Sea. After 5 h (01:00–06:00), most parts of the city experienced the influence of cold air in areas where cold air accumulated above 40 m. Cold air was most actively generated and flowed smoothly in the early morning; therefore, most parts of the study area experienced the influence of cold air after 6 h. The simulation results of the cold air height and flow range showed that the cold air generated after sunset flowed following the spatial characteristics of the terrain. Specifically, the cold air flow range quickly expanded along the stream (Hyeongsan River), indicating that the region could be a major wind corridor. The flow of cold air exhibited a similar pattern after the midpoint of the simulation, gradually expanding its range around the stream (Hyeongsan River). An analysis of the cold air height and flow range in Pohang indicated that the cold air height and flow range expanded around the Hyeongsan River, and the city center (Daei-dong, Jukdo-dong, and Songdo-dong) experienced the influence of cold air after 5 h.

A simulation analysis was conducted for the difference in cold air heights before and after the water curtains were installed on bridges (the POSCO and Hyeongsan Big Bridges) near the Hyeongsan River and the East Sea. After 1 h, the cold air on the inner side of the bridge (Hyeongsan) applied to the water curtain accumulated 1 m to 9 m higher than the heights observed before the scenario was applied, whereas the cold air on the outer side of the bridge (East Sea) accumulated 1 m to 4 m lower than the heights observed before the scenario was applied. After 2 h, this tendency became more apparent in areas where the range of influence had expanded to nearby towns. After 3 h, the cold air in the areas near the inner side of the bridge accumulated 10 m to 19 m higher than the heights observed before applying the scenario, whereas the cold air in the areas near the outer side of the bridge accumulated 10 m to 19 m lower than the heights observed before applying the scenario. After 4 h, an increase in the cold air height at the inner side of the bridge after applying the scenario was observed throughout the city, whereas a decrease in the cold air height at the outer side of the bridge was noted across a wide area. Overall, operating the water curtains installed on the bridges guided the cold air flowing along the Hyeongsan River toward the East Sea to spread to nearby urban areas.

Third, three observation points were selected on the inner and outer sides of the water curtain, and changes in cold air heights at these points before and after applying the water curtains were noted. The three observation points on the inner side were (A) Pohang Nam-gu Office (X:116,7571, Y:1,780,587), (B) Daedo Sageori (X:1,167,673, Y:1,781,700), and (C) Ogeori (X:1,168,120, Y:1,783,374). The three observation points on the outer side were (D) Pohang Inner Harbor Boat Dock (X:1,169,175, Y:1,782,384), (E) Pohang Meteorological Observatory (X:1,169,382, Y:1,783,319), and (F) East Sea (X:1,170,331, Y:1,783,743).

Fourth, a "wind-generating forest" refers to forests and green lands on the outskirts of a city, wherein cold air is generated at night and purified cold air blows; it includes most forests inside and outside the city. The total area of forests located inside and outside the city, corresponding to the wind-generating forest in the study area, was 374.9 km^2. The Unjesan, Sambongsan, Seongjeoksan, Johyangsan, and Doeumsan mountains are included in the area. A "connecting forest" refers to green lands that help the cold air generated in a wind-generating forest to flow into the city; it encompasses linear and belt greens, including roadside trees and stream banks. The total area of the green land facility inside the city corresponding to the wind-connected forests in the study area was 2.5 km^2. A total of 357 landscape green spaces, buffers, and other green spaces were included in the study. Roadside trees also belong to the connecting forest, but they were excluded from this study because of limitations in collecting relevant information space data. It may have resulted in a less comprehensive understanding of the overall ventilation dynamics within the study area, and it is essential to recognize this limitation to emphasize the need for future research to incorporate roadside trees into analyses for a more holistic understanding of urban ventilation systems. A "wind-spreading forest" refers to a base forest in a city that generates a breeze using the temperature difference in the city and forest areas; it includes the green lands within a city, e.g., public and rooftop parks and school forests. The total area of wind-spreading forests within the study area located inside and outside the city was 0.5 km^2. In total, 174 children's, neighborhood, and small parks were included in this study.

Fifth, the correlation analysis between cold airspeed and the urban wind-corridor forest area ratio indicated that the urban wind-corridor forest area increased as the GAR increased. The same trend was observed for the cold air speed of the grid. SPSS was used to perform a correlation analysis between cold airspeed and GAR. The Pearson correlation was measured after matching the GAR data with a grid with the cold air speed in the region. The GAR and cold air speed showed a positive correlation of +0.153.

Limitations and Implications

The accuracy and reliability of spatial data are key for ensuring the validity of analyses, particularly in studies assessing complex systems like urban forests. Given the study's reliance on spatial data to evaluate the structure and function of urban forests, any inaccuracies or errors within the data could significantly compromise the integrity of the analysis. Inaccurate data may lead to misleading conclusions and undermine the study's credibility. Therefore, it is essential to employ reliable data sources and rigorously validate the accuracy of spatial data. Furthermore, validation and calibration processes must be conducted to ensure the accuracy of the results, as conducted in the study by Seo and Jung (2017) [35], where the results of the KLAM_21 model were verified with measurements made with the Automatic Weather System (AWS), confirming the reliability of the numerical modeling analysis. While this study failed to conduct this validation process, it provides basic data for future study enhancement.

For future studies, further investigation into the role of roadside trees in urban wind corridors is needed. Since roadside trees were excluded from this study due to limitations in data collection, future research should focus on incorporating roadside trees into analyses to provide a more comprehensive analysis. This could include developing methods to accurately collect and analyze spatial data related to roadside trees and their influence on cold airflow. Similarly, the effectiveness of different types of urban green spaces in mitigating the UHI effect should be explored. This study identified wind-generating forests, connecting forests, and wind-spreading forests as key components of urban wind-corridor systems. Future research could delve deeper into the specific characteristics and functions of these different types of green spaces, examining their effectiveness in reducing the UHI effect and improving overall urban thermal environments. Lastly, given the correlation between urban wind-corridor forest area ratio and cold air speed identified in the study, future research could explore the potential of urban forest planning strategies, such as increasing the area of wind-corridor forests, in influencing local climate conditions. This could involve conducting empirical studies in various urban settings to evaluate the effectiveness of different forest planning approaches in promoting natural ventilation and enhancing urban thermal comfort.

While the study provides valuable insights into cold airflow patterns and their impact on UHIs, its limitation in conducting a deeper analysis across different seasons stems from its focus on a specific period (2013–2022) without discerning seasonal variations. Variability in climatic conditions across seasons, such as temperature gradients and wind patterns, can significantly influence cold air flow dynamics and the UHI effect. Thus, a more comprehensive understanding of these phenomena would require data spanning multiple seasons to capture seasonal trends and variations. Additionally, considering factors like changes in vegetation cover and land use patterns throughout the year could provide a more nuanced understanding of the dynamics driving the UHI effect and cold airflow patterns.

The proposed strategies in this study focus on optimizing wind corridors through forest management, green space development, and infrastructure improvements, presenting significant policy implications for urban planning and environmental management. By enhancing cold air production and circulation, these measures aim to mitigate the UHI effect and improve air quality, thereby reducing respiratory issues and heat-related illnesses among residents. Additionally, the installation of water curtains on bridges is suggested to guide cold air flow, further enhancing outdoor comfort and environmental quality. The correlation between the urban wind-corridor forest area ratio and cold air speed underscores the importance of urban forest planning in influencing local climate conditions. However, future research should explore the role of roadside trees and different types of urban green spaces in mitigating the urban heat island effect, considering seasonal variations and changes in vegetation cover.

6. Conclusions

In conclusion, the study provides valuable insights into cold airflow patterns and their impact on the UHI effect in Pohang City. By analyzing demographic and social environments, meteorological data, and simulation results, the study highlights the significance of evidence-informed urban planning strategies in mitigating the UHI effect and promoting environmental quality. Key findings suggest that optimizing wind corridors through forest management and green space development can effectively mitigate the UHI effect and improve air quality. Moreover, the installation of water curtains on bridges shows promise in guiding cold air flow, further enhancing outdoor comfort. However, future research should address the limitations of the study, including the incorporation of roadside trees and consideration of seasonal variations. By doing so, policymakers can develop more effective strategies to create healthier and more sustainable urban environments in Pohang City and beyond.

Author Contributions: Conceptualization, W.J. and G.K.; methodology, W.J. and G.K.; data curation, W.J.; writing—original draft preparation, W.J. and G.K.; writing—review and editing, W.J. and G.K.; visualization, W.J.; supervision, G.K.; project administration, G.K. All authors have read and agreed to the published version of the manuscript.

Funding: This work was supported by the National Research Foundation of Korea (NRF) grant funded by the Korea government (MIST) (No. NRF2022R1F1A107516111).

Data Availability Statement: The original contributions presented in the study are included in the article, further inquiries can be directed to the corresponding author.

Conflicts of Interest: The authors declare no conflicts of interest.

Appendix A

Table A1. Data sources and description.

Division		Data Source		Year	Spatial Resolution
KLAM_21	**Terrain**	U	https://map.ngii.go.kr/ accessed on 9 November 2023	2022	5 m
	Land cover	Environmental Spatial Information Service (Ministry of Environment)	https://egis.me.go.kr/ accessed on 18 December 2023	2021	1 m
	Building	Address-based industry support service (Ministry of the Interior and Safety)	https://business.juso.go.kr/ accessed on 6 December 2023	2022	5 m
	Weather	Weather Data Open Portal (Korea Meteorological Administration)	https://data.kma.go.kr/ accessed on 18 September 2023	2013–2022	-
Wind corridor	**Terrain**	National Land Information Platform (National Geographic Information Institute)	https://map.ngii.go.kr/ accessed on 3 August 2023	2022	5 m
	Forest	Forest Spatial Information Service (Korea Forest Service)	https://www.forest.go.kr/ accessed on 8 April 2023	2013	10 m
	Greenery	V-World Open Market (Ministry of Land, Infrastructure and Transport)	https://www.vworld.kr/ accessed on 1 Septemebr 2023	2022	5 m
	Park				
Etc.	**Hydrosphere**				

References

1. Kim, S.-B.; Jung, E.-H.; Lee, C.-W. A Study on the Review of Legislation and Practical Application to Establish Wind Corridor. *J. Environ. Sci.* **2007**, *12*, 127–143. [CrossRef]
2. Mosimann, T.; Frey, T.; Trute, P. Schutzgut Klima/Luft in der Landschaftsplanung. *Informationsdienst Naturschutz Niedersachs.* **1999**, *19*, 201–276.
3. Schädler, G.; Lohmeyher, A. *Kaltluft-und Windfeld-Berec hnungen fur den Raum Stuttgart im Zusammenhang mit der Planung fur das Projekt "STUTTGART21"*; Umweltschutz-und Ordnungsreferat, Amt für Umweltschutz, Abt. Stadtklimatologie: Stuttgart, Germany, 1996.
4. Kress, R. *Regionale Luftaustauschprozesse und ihre Bedeutung für die Räumliche Planung. Bonn-] Bad Godesberg: Bundesminister für Raumordnung, BAUWESEN und Städtebau*; Universität Dortmund: Dortmund, Germany, 1979.
5. Eum, J.-H.; OH, J.-H.; Son, J.-M.; Kim, K.; Baek, J.-B.; Yi, C.-Y. Analysis Schemes of Wind Ventilation Forest Types: A Case Study of Daegu Metropolitan City. *J. Korean Asoc. Geogr. Inf. Stud.* **2019**, *22*, 12–23. [CrossRef]
6. Kim, S.-B.; Jung, E.-H. Basic research on the introduction of wind roads for eco-friendly city construction. *Daegu Daegu Gyeongbuk Inst.* **2005**, *7*, 37.
7. Chandler, T.J. Absolute and relative humidities in towns. *Bull. Am. Meteorol. Soc.* **1967**, *48*, 394–399. [CrossRef]
8. Oke, T.R. *Boundary Layer Climates*; Routledge: London, UK, 1987.
9. Wang, W.; Wang, D.; Chen, H.; Wang, B.; Chen, X. Identifying urban ventilation corridors through quantitative analysis of ventilation potential and wind characteristics. *Build. Environ.* **2022**, *214*, 108943. [CrossRef]
10. Gholipour Gashniani, M.; Yazdani, D. Studying the usage of Double Skin Facades in utilizing Manjil wind in building ventilation. *J. Renew. New Energy* **2022**, *9*, 110–118.
11. Gu, K.; Fang, Y.; Qian, Z.; Sun, Z.; Wang, A. Spatial planning for urban ventilation corridors by urban climatology. *Ecosyst. Health Sustain.* **2020**, *6*, 1747946. [CrossRef]

12. Marando, F.; Heris, M.P.; Zulian, G.; Udías, A.; Mentaschi, L.; Chrysoulakis, N.; Parastatidis, D.; Maes, J. Urban heat island mitigation by green infrastructure in European Functional Urban Areas. *Sustain. Cities Soc.* **2022**, *77*, 103564. [CrossRef]
13. Son, J.-M.; Eum, J.-H.; Kim, S. Wind corridor planning and management strategies using cold air characteristics: The application in Korean cities. *Sustain. Cities Soc.* **2022**, *77*, 103512. [CrossRef]
14. Sung, U.-J.; Eum, J.-H.; Son, J.-M.; Oh, J.-H. Planning Strategies of Wind Corridor Forests Utilizing the Properties of Cold Air. *Land* **2021**, *10*, 607. [CrossRef]
15. Cha, J.-G. The Analysis and Evaluation on the Changes in Wind Flow from a Different Land Use. Ph.D. Thesis, Keimyung University, Daegu, Republic of Korea, 2010.
16. Seo, B.-Y. A Study on Cold Air Flow from Development of Apartment Housings and Legal and Institutional Development Measures: Focusing on Daegu Yeongyeong Public Housing District. Ph.D. Thesis, Keimyung University, Daegu, Republic of Korea, 2022.
17. Kim, S.-B.; Jung, E.-H.; Kim, Y.-B. A Study on An Installment of Cool Corridors Reducing Urban Heat Island Phenomenon in Daegu, Korea. *J. Nakdonggang Environ. Res. Inst.* **2004**, *9*, 143–156.
18. Eum, J.-H. Analysis and Utilization Strategies of Ventilation Corridor Characteristics in Jeon-ju Area. *Korean J. Environ. Ecol.* **2019**, *33*, 366–374. [CrossRef]
19. Kim, J.-S.; Kang, J.-E. A Study on the Effectiveness of Wind Corridor Construction for Improving Urban Thermal Environment: A Case study of Changwon, South Korea. *J. Environ. Impact Assess.* **2021**, *30*, 187–202. [CrossRef]
20. Moon, H.-Y.; Gweon, Y.-D.; Park, H.-B. Ventilation Corridor Characteristics Analysis and Management Strategy to Improve Urban Thermal Environment: A Case Study of the Busan, South Korea. *Korean J. Environ. Ecol.* **2021**, *35*, 659–668. [CrossRef]
21. Lin, J.; Wei, K.; Guan, Z. Exploring the connection between morphological characteristic of built-up areas and surface heat islands based on MSPA. *Urban. Clim.* **2024**, *53*, 101764. [CrossRef]
22. Zheng, Y.G.; Han, Q.; Keeffe, G. An evaluation of different landscape design scenarios to improve outdoor thermal comfort in Shenzhen. *Land* **2024**, *13*, 65. [CrossRef]
23. Lin, Z.; Xu, H.; Yao, X.; Yang, C.; Yang, L. Exploring the relationship between thermal environmental factors and land surface temperature of a "furnace city" based on local climate zones. *Build. Environ.* **2023**, *243*, 110732. [CrossRef]
24. Jung, J.-H.; Lee, H.-D.; Son, B.-H. Assessment of location of the air quality monitoring stations according to the analysis of wind sector division in Pohang. *J. Korea Acad.-Ind. Coop. Soc.* **2012**, *13*, 1931–1938. [CrossRef]
25. Sievers, K. The cold air drainage model KLAM_21—Model formulation and comparison with observations. *Weather Clim.* **2016**, *36*, 2. [CrossRef]
26. Wang, Z.; Li, Y.; Song, J.; Wang, K.; Xie, J.; Chan, P.W.; Ren, C.; Di Sabatino, S. Modelling and optimizing tree planning for urban climate in a subtropical high-density city. *Urban. Clim.* **2022**, *43*, 101141. [CrossRef]
27. Huang, H.; Yang, H.; Chen, Y.; Chen, T.; Bai, L.; Peng, Z. Urban green space optimization based on a climate health risk appraisal—A case study of Beijing city, China. *Urban. For. Urban. Green.* **2021**, *62*, 127154. [CrossRef]
28. Jiang, Y.; Song, D.; Shi, T.; Han, X. Adaptive analysis of green space network planning for the cooling effect of residential blocks in summer: A case study in Shanghai. *Sustainability* **2018**, *10*, 3189. [CrossRef]
29. Altunkasa, C.; Uslu, C. Use of outdoor microclimate simulation maps for a planting design to improve thermal comfort. *Sustain. Cities Soc.* **2020**, *57*, 102137. [CrossRef]
30. Gu, J.; Liu, H.; Lu, H. Can Even a Small Amount of Greenery Be Helpful in Reducing Stress? A Systematic Review. *Int. J. Environ. Res. Public Health* **2022**, *19*, 9778. [CrossRef] [PubMed]
31. Emmanuel, R.; Loconsole, A. Green infrastructure as an adaptation approach to tackling urban overheating in the Glasgow Clyde Valley Region, UK. *Landsc. Urban Plan.* **2015**, *138*, 71–86. [CrossRef]
32. James, P.; Banay, R.F.; Hart, J.E.; Laden, F. A Review of the Health Benefits of Greenness. *Curr. Epidemiol. Rep.* **2015**, *2*, 131–142. [CrossRef]
33. Ulpiani, G.; Di Giuseppe, E.; Di Perna, C.; D'Orazio, M.; Zinzi, M. Thermal comfort improvement in urban spaces with water spray systems: Field measurements and survey. *Build. Environ.* **2019**, *156*, 46–61. [CrossRef]
34. Ulpiani, G.; Di Perna, C.; Zinzi, M. Water nebulization to counteract urban overheating: Development and experimental test of a smart logic to maximize energy efficiency and outdoor environmental quality. *Appl. Energy* **2019**, *239*, 1091–1113. [CrossRef]
35. Boyong, S.; Jung, E. Comparative analysis of wind flows in wind corridor based on spatial and geomorphological characteristics to improve urban thermal environments. *J. Korean Assoc. Geogr. Inf. Stud.* **2017**, *20*, 75–88. [CrossRef]